Ana Sofia Martins Roda

BSc in Biochemistry

Nanoparticles for recognition and delivery in metastatic colorectal cancer cells

Dissertation for the Master degree in Biochemistry for Health

Supervisor: Arturo Álvarez-Bautista, PhD, iBET
Co-supervisor: Catarina Duarte, PhD, iBET

Setembro, 2016

Ana Sofia Martins Roda

BSc in Biochemistry

Nanoparticles for recognition and delivery in metastatic colorectal cancer cells

Dissertation for the Master degree in Biochemistry for Health

Supervisor: Arturo Álvarez-Bautista, PhD, iBET
Co-supervisor: Catarina Duarte, PhD, iBET

Instituto Tecnológico de Química e Biologia (ITQB NOVA)

Setembro, 2016

[Nanoparticles for recognition and delivery in metastatic colorectal cancer cells]

'A vida está em constante mudança'

'A vida está em constante evolução'

Não saiba eu outra coisa…

Mas quero saber mais,

Quero evoluir mais!

Quero viver a vida e que ela viva comigo

Estou adsorvida à sua superfície e vou avançar,

E absorver a mim tudo o que ela tiver para me dar!

AGRADECIMENTOS

Em primeiro lugar quero agradecer ao meu orientador, Dr. Arturo Álvarez Bautista pela oportunidade de integrar este plano de dissertação de mestrado e por todo o apoio e formação prestada no decorrer da tese, bem como a sua humildade e constante preocupação para comigo. Teve sem dúvida uma contribuição muito valiosa, tanto a nível profissional como pessoal. Obrigada.

À minha co-orientadora, Drª Catarina Duarte, quero agradecer pela sua importante contribuição na escolha desta dissertação, pelo conhecimento que partilhou e pela sua vocação para a ciência, inspiradora e contagiante, instruindo sempre no sentido da evolução. Um especial apreço pela sua humildade e pela sua coragem. Palavras para quê?. Seja sempre a pessoa fantástica que é.

A todos os membros que integram ou integraram o grupo dos Nutracêuticos e Libertação Controlada, agradeço pela receção e integração no grupo e pelo apoio prestado a todos os níveis. Um especial obrigado à Maria João, Luís Martins, Daniel Deodato, Agostinho e Liliana Rodrigues, que despenderam do seu tempo para me auxiliar em diversas ocasiões. Quero também agradecer à Drª Teresa Serra e Drª Ana Matias cuja postura e envolvimento no grupo contribuiu para o decorrer do projeto, nas melhores condições possíveis. E como não podia deixar de ser, às minhas companheiras e colegas de mestrado e do grupo, Joana Guerreiro, Carolina Pereira e Lucília Pereira. Em especial à minha colega e agora amiga, Anyse Pereira, que me acompanhou, lado a lado, em todos os momentos. Obrigada por teres entrado na minha vida e por contribuíres para o meu bem-estar e para minha evolução pessoal.

Ainda no contexto do mestrado, não posso deixar de agradecer a todos os grupos e pessoas que direta ou indiretamente, tornaram possível a concretização da parte experimental da tese. Em especial, às colaborações do grupo 'Homogeneous catalysis' (Drª Beatriz Royo, ITQB), à Drª Isabel Nogueira (IST), ao grupo do professor João Paulo Crespo (FCT/UNL) e por fim, ao 'Colon Pathology Study Group' (Cristina Albuquerque, IPO), envolvido em parceria no projeto e cuja contribuição foi crucial. Para além disso, também a professora Teresa Catarino e o professor Pedro Matias merecem um especial agradecimento, pelo seu profissionalismo enquanto coordenadores de mestrado, pelo seu interesse e constante preocupação por manter-nos sempre informados e pela vontade de acompanhar e contribuir para o nosso percurso.

O agradecimento mais importante dirige-se aos meus pais, que com muito esforço tornaram possível esta oportunidade. Muito obrigado. A toda a minha família, obrigada por contribuírem para a pessoa que sou, em especial aos meus tios, Luís Martins e Carla Firmo, que desde cedo me motivaram e me instigaram a evoluir e sempre se mostraram interessados e disponíveis. São sem dúvida, um modelo de inspiração.

A todos os meus amigos, obrigada por serem o meu pilar nesta jornada. Inês Brito, Paulo Oliveira, Khrystyna Kucheryava, não tenho palavras para descrever a vossa contribuição. Obrigada pela vossa amizade, pelo vosso apoio incondicional, adoro-vos. Diana Silva, obrigada pela tua energia, sempre positiva e contagiante.

Às minhas quatro e para sempre amigas, Ana Raquel Maia, Ana Sofia Narciso, Ana Paulino e Maria Inês Marreiros. Obrigada pela longa e fiel amizade.

Daniel Vilar Jorge, a ti um especialíssimo obrigado, pela tua amizade, pelo teu conhecimento, pela tua disponibilidade e pelo teu apoio incondicional.

Catarina Silva. És tu, somos nós! Não preciso de dizer mais nada. Adoro-te.

Rúben Santos, mereces um grande obrigado, pela tua amizade e por me incentivares e te disponibilizares a ajudar-me nesta fase tão importante.

Miguel Mataloto, entraste de rompante, mas vens para ficar. Obrigada por tudo.

Abstract

Colorectal cancer is a global health concern. The high incidence of colorectal metastasis, mainly in the liver, triggers an increase of the mortality rate and greatly reduces the effective cure chances. For this reason, the investigation in the area is now focused on efficient detection and elimination of metastasis. Nanotechnology has become a fundamental research field since it provides promising perspectives regarding specific, oriented and sustained delivery of loaded nanoparticles for nanoteragnostic approaches. The current project aims to develop a nanocarrier, strategically constructed for specific administration, recognition and therapy of colorectal liver metastasis. Concerning this goal, two different approaches were concurrently developed: a green-therapeutic technology and a novel nanoparticulate system, by nanoprecipitation and inverse microemulsion, respectively. The green approach focused on the encapsulation of a natural anticancer agent, phenetyl isothiocyanate (PEITC) in methoxy polyethylene glycol-co-poly ε-caprolactone (mPEG-co-PCL) nanoparticles. The development of this system did not advance significantly since more promising perspectives in a shorter period of time were obtained for the simultaneous developments of chitosan-collagenase nanosystems. Chitosan-collagenase NPs were designed and developed for the first time due to their innovative properties regarding specificity in drug delivery and release. These nanosystems presented spherical shape and sizes in the range of 100 to 500 nm. The studies of pH and crosslinking influence in network swelling suggested higher swellings for more acidic pH and lower crosslinker contents. It was also postulated that the crosslinking degree influences differently the loading capacity and release efficiency of nanoparticles. As nanocarrier, chitosan-collagenase NPs demonstrated acceptable loads of the chemotherapeutic agent 5-fluorouracil for *in vitro* tests in HT29 cell lines but low release efficiencies.

Keywords: metastatic colorectal cancer; polymeric nanoparticles; drug delivery; mPEG-co-PCL; chitosan; collagenase

Resumo

O cancro coloretal é a terceira causa mundial de morte por cancro. A alta incidência de metástases, sobretudo no fígado, impulsiona a sua taxa de mortalidade e reduz substancialmente as hipóteses de cura. Por esse motivo, a investigação na área está focada na deteção e eliminação eficiente de metástases. A nanotecnologia tem demonstrado perspetivas promissoras no desenvolvimento de nanosistemas para libertação dirigida, controlada e continuada de agentes encapsulados para nanoteragnóstico. O presente trabalho tem como objetivo alargado o desenvolvimento estratégico de nanopartículas para administração, reconhecimento e terapia especializada do cancro coloretal metastático. Nesse intuito, foram desenvolvidos simultaneamente dois sistemas nanoparticulados. Uma abordagem ecológica focou a encapsulação de um agente anticancerígeno natural, PEITC, em mPEG-co-PCL, por nanoprecipitação. Até ao momento, o desenvolvimento deste nanosistema não avançou significativamente. Paralelamente, nanopartículas de quitosano-collagenase foram projetadas e desenvolvidas pela primeira vez por microemulsão inversa, devido às suas propriedades potenciais na otimização de terapêuticas. Estes nanosistemas revelaram morfologia esférica, com tamanhos na ordem dos 100 aos 500 nm. Os estudos da influência do pH e do grau de entrecruzamento no inchamento das redes nanoparticuladas sugeriram maiores inchamentos com o aumento de acidez e diminuição de entrecruzante. Postulou-se também que o aumento de entrecruzante confere à rede nanoparticulada maior capacidade de encapsulação e menor eficiência de libertação. A encapsulação de 5-fluorouracil demonstrou ser aceitável para testar em linhas celulares HT29, apesar da obtenção de baixas eficiências de libertação.

Palavras-chave: cancro colorectal metastático; nanopartículas poliméricas; libertação de fármacos; mPEG-co-PCL; quitosano; colagenase

CONTENTS

FIGURE INDEX

TABLE INDEX

1. OBJECTIVES AND FRAMEWORK

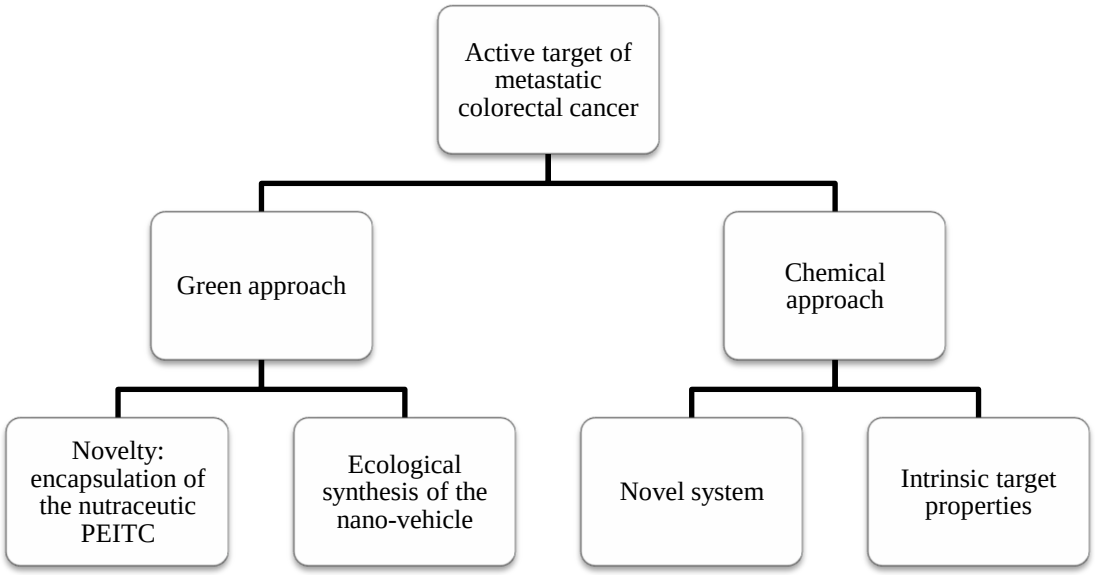

Figure 1.1 – Schematic representation of the thesis major goal and the designed approaches and its advantages for the purpose.

The work developed during this master thesis is part of a project with higher scope, evaluated, approved and financed by iNOVA4health, as a promising translational program for advanced precision medicine. With a three year initial timetable, it has the final goal of obtaining specific nanoparticulate therapeutic systems for differential recognition of the several forms of metastatic colorectal cancer.

The master thesis focused on **liver metastatic colorectal cancer**, the most common metastasized site. The predicted tasks included the synthesis, characterization and functionalization of two parallel systems, with polymeric composition but different designs. One pathway was directed to a green approach, by using a clean and sustainable methodology for the encapsulation of two, independent agents, the coumarin – 6 (C6), a fluorescent marker used for imaging and phenetyl isothiocyanate (PEITC), a natural therapeutic drug. PEITC was chosen mainly due to its nutraceutical nature, contributing to a chemopreventive/chemotherapeutic green approach. In turn, since C6 is an agent with published results regarding its incorporation in mPEG-co-PCL system, its encapsulation was reproduced for comparative purposes with literature. Besides, its fluorescent properties can be potentially used for monitoring of nanoparticles during *in vitro* delivery assays.

As further explained below, methoxy poly (ethylene glycol) nanocarriers were chosen mainly because of their ‘green’, fast and simple synthesis procedure, well described by several authors in the literature and considered reliable, reproducible and adequate for pharmaceutical application. The

reproduction of the published results would allow us to obtain monodisperse ecologic nanosystems whose composition would be immediately ready to perform functionalization studies without additional surface modifications. Besides, the quick synthesis would enable to initiate the functionalization assays in early stages, allowing the test and optimization of several biomarkers and its specificity for colorectal metastatic cancer.

Concurrently, a potentially innovative chemical approach to obtain a novel system was designed based on the nano-combined advantages of chitosan and collagenase compounds. It is expected to form a promising drug vehicle mainly due to its intrinsic biomarker properties, deeper penetration ability and pH response, which translates into selective accumulation in metastatic cancer cells, allows to reach the tumour inner core, and the drug delivery occurs preferentially in acidic tumoral pH. Moreover, since it was expected to functionalize nanoparticles surface to target metastatic colorectal cancer, the load capacity and release efficiency of this system was planned to be tested using a commonly chemotherapeutic agent applied in the treatment of this type of cancer, 5-fluorouracil, for further *in vitro* assays in colorectal cancer cell lines.

Following this framework, the thesis structure will be divided into five main sections, Introduction, Experimental Section, Results and Discussion, Conclusions and Future work. The introductory section will first focus on the state of the art of colorectal cancer and nanotechnology, which are the bases of the project, then funnelling to the thematic contextualization of the principal materials involved in the project. The experimental section will contain a full description of the materials and procedures used. The section of results and discussion contains the outcomes of the experimental work developed as well and its evaluation, founded on the basis of literature available knowledge and expected results by comparative analysis. The Conclusions section will summarize the main outcomes of the experimental work and the future predicted tasks and further perspectives of the project will be summarized in the section of Future work.

PROJECT MAIN GOALS:

The main goal of this project was the synthesis and characterization of polymeric nanoparticles (PNPs) with nanometric size for parental administration of therapeutic drugs and further functionalization with specific markers for hepatic metastatic colorectal cancer.

2. INTRODUCTION

2.1. Colorectal cancer epidemiology

Colorectal cancer is a global health concern, with an incidence rate rising over the years. In 2012, presented an incidence of 1,36 million new cases, being the third cause of cancer death worldwide (Cancer Research UK, 2012). Regarding Europe, colorectal cancer represents the second position in terms of cancer occurrence and mortality, with register of about 447,000 cases and 215,000 deaths. In Portugal, it is also the second most common and lethal cancer, with an estimated prevalence of about 7130 cases and 3800 deaths (Ferlay et al., 2013). The late diagnosis, which often occurs in advanced stages of the disease, mainly metastatic, severely contributes to the current mortality rates. The hepatic colorectal cancer metastasis is the most frequent (Masi et al., 2011).

2.1.2. Conventional therapies

… colorectal metastasis as a 'stone' on the path to healing.

The available therapies are used for cancer treatment in general, presenting low specificity and efficiency. The most common therapy applied to treat colorectal cancer is surgery which comprises surgical removal of the tumour and part of the contiguous healthy tissue. However, it is not efficient in advanced stages of the disease and not applicable in cases where the removal can compromise the organ function. There are other therapies aiming at the reduction or eradication of the tumour and/or metastasis but all of the available treatments have the disadvantage of affecting healthy cells.

Chemotherapy consists on the intravenous administration of anticancer agents, having a systemic effect, which causes several collateral effects. Besides, the cells can become resistant to the drugs, compromising the efficiency of the treatment.

Radiotherapy is mainly applied as adjuvant and despite being based on local administration of high energy radiation, has similar drawbacks regarding secondary effects and resistance.

On the other hand, ablation is based on local destruction by injection of a needle/probe into the tumour as source for direct treatment, but it is only efficient for small tumours or metastasis. Embolization can be applied for larger tumours/metastasis in the liver and consists on blocking the branches of the hepatic artery, since it is the main blood source of liver cancer cells. Despite the fact that normal cells remain supplied by the portal vein, the blood supply of liver tissue is reduced, which can affect its normal function.

The invasive effect of most of these treatments translates into a debilitated health for life. However, the cure of a primary tumour is achievable, normally by resection (Colorectal Cancer, American Cancer Society). The incurability of the disease is mainly related to the difficulty of

metastasis eradication. Normally, it is possible to control its progression for a certain period, but considering the present and reachable developments, prolonging patient's life is for now, the only achievable goal. Scientific efforts are focused on countering the inability of curing this disease, aiming to achieve efficient, long-term survival and non-pejorative treatments (Masi et al., 2011; Raval et al., 2014; van Hazel et al., 2016).

2.2. Nanotechnology

'There's plenty of room at the bottom' (Richard Feynman, 1959)

In the past decades, nanotechnology has arisen as a potential alternative to overcome the issues faced by the conventional medicine, regarding both diagnosis and therapy. The combination of nanoscale properties and cancer characteristics, allows by itself a preferential accumulation of nanosystems in the tumour environment (passive targeting), mainly due to the Enhanced Permeability and Retention (EPR) effect. The enhanced permeability in comparison with normal capillary systems occurs due to the leaky and defective vasculature of the tumours as a result of the extra and accelerated vascularisation in response to the nutritional needs required for the proliferative ability of cancer tissues. This phenomenon translates into gaps in the surrounding vessels, leading to extravasation of nanoparticles into cancer cells interstitium, whose retention is ensured by the characteristic absence of lymphatic drainage (Sinha et al., 2006).

In addition to the intrinsic EPR effect, there are other passive targeting strategies that can be applied to further specify the nanoparticles delivery, either by localized administration or by manipulating the nano formulation according to intrinsic characteristics of the delivery pathway. Regarding colorectal passive targeting, the main influences relate to gastrointestinal physiology, including pH, temperature, ionic strength, enzymes, mucoadherence and tumour microenvironment (Patel Parul, Satwara Rohan, & Pandya, 2012). Besides, there are active targeting approaches, based on delivery driven by functionalization with biomarkers, which restricts the distribution according to the specificity. The advanced state of investigation and exponential growth in molecular and genetic biology allows the identification of potential sensitive biomarkers and increasingly confined probes. This knowledge is very useful regarding the development of highly specific systems in terms of differential recognition, conferring strong specificity and efficiency to diagnosis and therapy approaches.

2.2.2. Nanotechnology scale

The size range defined for nanoparticles is commonly 1 to 100 nm, according to the ISO (International Organization for Standardization) and ASTM International (American Society for Testing and Materials) standards. However, it is not possible to define unequivocal size limits since the physicochemical properties vary with the materials and surrounding conditions as well as its size dependence. Whereas the characteristics are acceptable under the predicted safety and risk parameters, and as long as the size is adequate and favourable for the application, the nano size range can be adjusted. Currently, according to the SCENIHR (Scientific Committee on Emerging and Newly Identified Health Risks), the standards remain ambiguous, being established differently, according to the area, material and application.

Regarding formulations for health purposes, it is important to ensure a sufficient residence time in the system to enable effective action. In this sense, the lower size limit for nanoparticles should be higher than 6 nm to prevent rapid renal clearance and above 15 nm to allow accumulation in liver and spleen, if required (Choi et al., 2007).

Another application with limited size required is internalization of nanoparticles in cells. Despite depending on many other factors as charge, shape and composition, the nanoparticles size greatly influences the occurrence and effectiveness of the cell uptake. For most cases, cellular internalization is described to occur up to 100 nm, with a maximum uptake varying from 50 to 100 nm (Shang, Nienhaus, & Nienhaus, 2014). However, there are some exceptions, as in the case of polymeric nanoparticles, for which there are published results that refer cell internalization of larger nanoparticles (until 500 nm) (Rejman et al., 2004; Shang, Nienhaus, & Nienhaus, 2014).

2.3. Anticancer reduced scale approved therapies

…if the wings of a butterfly can cause a hurricane, imagine what nanoscale can achieve.

In terms of current or ‘in test’ applications, the main approach is to use nanotechnology has bypass vehicle for the available or innovative therapies, using the nanosystems properties has an advantage. The most common application is the use of these systems for drug delivery, by active or passive targeting. The first approved nano-formulation by FDA (Food and Drug Administration) for this purpose, was Doxil, in 1995, a liposomal vehicle with a size range of 80 to 90 nm for the delivery of doxorubicin to treat metastatic ovarian cancer and AIDS (Acquired Immune Deficiency Syndrome)-related Kaposi’s sarcoma. All the approved and marketed anticancer nanoformulations to date are summarized in Table 2.1, and the current clinical trials for the same purpose are shown in Table 2.2. Most of the developments were based on lipossomal formulations as the optisomal technology, a 100 nm sphingomyelin/cholesterol liposome vehicle, with is first FDA approval in 2012 (Marqibo) for

vincristine delivery against Philadelphia chromosome-negative acute lymphoblastic leukemia. Two parallel systems using this technology, Alocrest and Brakiva, are currently in phase I clinical trials, for chemotherapeutic applications through vinorelbine and topotecan agents, respectively. Alocrest is being tested for breast and non-small cell lung cancer and Brakiva in non-small cell lung cancer, myelodysplastic Syndromes, ovarian cancer and acute myeloid leukemia.

The most recent anticancer FDA approved nanoformulation (2015) was Onivyde, also known as MM-398 or PEP02. It has been revised and marketed in 2015 from its first U.S approval in 1996. It is indicated for metastatic pancreatic cancer therapy, in combination with fluorouracil and leucovorin. Besides, is also involved in phase II clinical trials for colorectal cancer, gastric cancer and glioma and in phase I clinical trial for solid tumours.

In addition to the targeting ability, the systems composition can be modulated to be sensitive or responsive to a certain detection or therapy application, by external stimuli. In these cases, besides the vehicle ability, they can be involved in the diagnostic or therapeutic procedure. A therapy example is the SIRT (Selective Internal Radiation Therapy), which uses modulated systems with metallic specific characteristics to direct the treatment into an unique area, where those systems are preferentially accumulated. An approved SIRT approach is the administration via hepatic artery of microbeads coated with isotope yttrium-90 (Y-90) for pancreatic and hepatic liver cancer therapy, commercially available as TheraSpheres (20–30 μm spheres from BTG International Canada Inc) and SIR-spheres with 20-60 μm, prepared by Sirtex Medical Inc.

The most recent commercialized therapy with responsive characteristics is NanoTherm, with regulatory approval by European Union since 2010, recently (2016) marketed in Germany to treat brain tumours by thermal ablation. These 15 nm aminosilane-coated superparamagnetic iron oxide nanoparticles are in active expansion, with near perspectives of commercialization in European Union. Additionally, the treatment has been adapted to prostate cancer and submitted to FDA as an Investigational Device Exemption. The modulated Nanotherm devices for treating both prostate and brain cancer are now undergoing preclinical studies in the USA.

A nanosystem can have both active and passive contributions in a treatment, when combining the encapsulating ability with sensitive therapeutic properties to external stimuli, being a therapy vehicle and part of the treatment itself. A good example is ThermoDOX, a lysolipid thermally sensitive liposome encapsulating doxorubicin, which combined with thermal therapies, enhances its efficiency, both thermic and chemotherapeutic by localizing the heat (tumoral deeper penetration) and enhancing the drug liberation (improved release by lipossomal heating)

In terms of diagnosis approaches, the only nanoparticulate system with FDA approval and clinical application (2001, Europe; 2002, Japan) was Resovist (Ferucarbotran), superparamagnetic iron oxide nanoparticles, with 120 to 180 nm, administrated as contrast/imaging agents for magnetic

resonance imaging (MRI). However, the product has been discontinued in Europe by the Bayer Pharma AG distributer, being marketed only by I'rom Pharmaceutical Co Ltd, Japan (Baetke, Lammers, & Kiessling, 2015; Haegele et al., 2014).

2.3.2. Nanotherapies for colorectal cancer

…personalized therapies are the future.

Concerning the major therapeutic target of this thesis, hepatic metastatic colorectal cancer, there is a FDA-approved nanotherapy regarding the adjuvant application of both Y-90 SIRT (Selective Internal Radiation Therapy using yttrium-90 - SIR-spheres) and chemotherapy (Raval et al., 2014) and published and ongoing phase trials of variants of the same goal (van Hazel et al., 2016). Additionally, there are nanoformulations in clinical phase trials. The ThermoDOX, a heat-activated liposome technology, is currently in phase II clinical trials for combined administration with HIFU (High-Intensity Focused Ultrasound) in liver metastasis (and breast cancer) (Celsion Corporation). Other liposome-based formulation, containing a cisplatin analogue, is Aroplatin, in phase II development for intravenous chemotherapy of metastatic colorectal cancer. In turn, NK012 is a nanopolymeric micelle of PEG-polyglutamate copolymer incorporating SN-38, the active metabolite of irinotecan, currently in phase II studies for several cancers, including colorectal cancer (Ganji et al., 2015; Jin, Jin, & Hong, 2014; Raval et al., 2014).

Considering the epidemiology of metastatic colorectal cancer, much effort is concentrated on finding alternative therapies to reduce mortality. In terms of nanotherapies regarding this application, there are many other formulations in preclinical trials or in current development but not yet ready for clinical evaluation.

Table 2.1 - List of approved and marketed nanoparticulate systems for cancer therapy (updated to August 2016).

Nanoparticulate system	Commercial name	Drug/Active ingredient	Size range (nm)	Application	First year of approval
Pegylated liposomal doxorubicin	Doxil (Johnson & Johnson, USA) Caelyx (Janssen-Cilag, Europe) Evacet (Liposome company INC.,) Lipodox (Sun Pharma)	Doxorubicin (Adriamycin)	80-90	Metastatic ovarian cancer HIV-related Kaposi sarcoma	FDA, 1995
Liposomal Daunorubicin	Daunoxome	Daunorubicin	≈ 45	HIV-related Kaposi sarcoma	FDA, 1996
Cytarabine liposome	DepoCyt	Cytarabine	3000-30000	Lymphomatous meningitis	FDA, 1999/2007*

(continued)

Table 2.1 (continued)

Nanoparticulate system	Commercial name	Drug/Active ingredient	Size range/ nm	Application	First year of approval
Non-pegylated liposomal doxorubicin citrate	Myocet	Doxorubicin hydrochloride	≈180	Metastatic breast cancer, plus cyclophosphamide.	FDA, 2001 (Europe & Canada)
Microspheres Radionuclide/ yttrium-90 glass microspheres	TheraSpheres	Yttrium-90	20000-30000	Pancreatic and hepatic liver cancer	FDA, 1999
	SIR-Spheres	Yttrium-90	20000-60000	Liver metastatic colorectal cancer plus floxuridine	FDA, 2002
Tripartite viral particle	Rexin-G	Vector dnG1/C-REX	≈180	Pancreatic cancer	FDA orphan status, 2003
				Chemotherapy-resistant solid malignancies	Accelerated FDA Philippines approval, 2007
				Soft tissue sarcoma and osteosarcoma	FDA orphan status, 2008
Albumin-bound Paclitaxel	Abraxane	Paclitaxel	≈ 130	Metastatic breast cancer	FDA, 2005
				Advanced NSCLC	FDA, 2012
				Late-stage pancreatic cancer	FDA, 2013
PEG-asparaginase (Pegaspargase)	Oncaspar	L-asparaginase	50-200	ALL	Initial US approval:1994 FDA (revised), 2006
Micellar diblock copolymeric paclitaxel	Genexol-PM (Samyang, Korean) Cynviloq (Sorrento Therapeutics, Inc. and IGDRASOL, Europe)	Paclitaxel	20-50	Metastatic breast cancer, NSCLC and ovarian cancer	Approved and marketed in Korean (2007) Commercialized in Europe
Liposomal mifamurtide muramyl tripeptide phosphatidyl ethanolamine	Mepact	Mifamurtide	1000-5000	Osteosarcoma	Orphan medicinal product, 2004 Marketing authorization by EMA and European Commission (EU), 2009
Aminosilane-coated superparamagnetic iron oxide nanoparticles	NanoTherm	-	15	Thermal ablation in brain tumours	Regulatory approval from EU, 2010 Commerciallized in Germany, 2016
Liposomal vincristine sulphate/ Optisomal Vincristine	Marqibo (Onco TCS)	Vincristine	~100	Philadelphia chromosome-negative ALL	FDA, 2012

Table 2.1 (continued)

Nanoparticulate system	Commercial name	Drug/Active ingredient	Size range (nm)	Application	First year of approval
Paclitaxel micellar - Oasmia Pharmaceuticals (OAS-PAC-100/ Paclitaxel-XR-17)	Paclical/ Apealea	Paclitaxel	20-60	Ovarian cancer	Marketed in Russia and CIS, 2015 Orphan status, (EMA-2006; FDA-2009) (Marketing registration in EMA and FDA, 2016)
Irinotecan nanoliposome	Onivyde/ MM-398/ PEP02	Irinotecan	≈ 110	Metastatic pancreatic cancer, in combination with fluorouracil and leucovorin	Initial US approval:1996 FDA (revised), 2015 EMA and FDA Orphan status, 2011

Note:*Year of accelerated approval and full approval, respectively.

Abbreviations/Acronyms: FDA, Food and Drug Administration; EMA, European Medicines Agency; HIV, human immunodeficiency virus; PEG, polyethylene glycol; NSCLC, non-small cell lung cancer; ALL, acute lymphoblastic leukaemia; TNF, tumour necrosis factor; USA/US, United States of America; EU, European Union; CIS, Commonwealth of Independent States

References: (Baetke et al., 2015; Haegele et al., 2014; Hafner et al., 2014; Hang, Cooper, & Ziora, 2016; Jin et al., 2014; Pillai, 2014; Raju et al., 2015; Raval et al., 2014; Sanna, Pala, & Sechi, 2014; van Hazel et al., 2016; Ventola, 2012; Weissig, Pettinger, & Murdock, 2014) and the corresponding and supplementing sources (FDA, EMA and pharmaceutical companies' websites)

Table 2.2 - List of nanoparticulate systems for cancer therapy in current clinical trials (updated to August 2016).

Nanoparticulate system	Drug/Active ingredient	Potential application	Phase Trial
ThermoDOX	Doxorubicin (Adriamycin)	Primary Liver Cancer (mutual radiofrequency ablation)	Clinical Phase III (FDA Orphan Drug Status, 2009; Fast Track designation)
		RCW breast cancer (plus local hyperthermia)	Clinical Phase II
		Liver metastasis and breast cancer (plus HIFU)	Clinical Phase II
Paclitaxel Polyglumex/ Opaxio/ Xyotex/CT 2103	Paclitaxel	Ovarian cancer	Clinical Phase III
		Advanced NSCLC	Clinical Phase III (Fast Track designation, FDA)
		Malignant brain cancer (mutual Temozolomide and Radiotherapy)	Clinical Phase II (FDA Orphan Drug Status, 2012)
		Advanced esophageal cancer	Clinical Phase II

Table 2.2 (continued)

Nanoparticulate system	Drug/Active ingredient	Potential application	Phase Trial
Lipoplatin (Lipossomal cisplatin, Nanoplatin for NSCLC)	Cisplatin	NSCLC adenocarcionomas	Clinical Phase III
		Pancreatic cancer	Clinical Phase II/III (EMA Orphan Drug Status, 2007)
		Breast cancer; Gastric cancer	Clinical Phase II
		Malignant pleural effusion	Clinical Phase I
Micelplatin/Nanoplatin/NC-6004 (Cisplatin polymeric micellar nanoparticles)	Cisplatin	Pancreatic cancer	Clinical Phase III
		Bile duct cancer; Bladder cancer; NSCLC	Clinical Phase II
		Head and neck cancer	Clinical Phase I/II
CPX351/ Vyxeos (Lipossomal cytarabine:daunorubicin)	Cytarabine: Daunorubicin (5:1)	AML	Clinical Phase III (Orphan Drug Status – FDA, 2008; EMA-2012) Breakthrough Therapy and Fast Track status, FDA)
NK105 (Paclitaxel micelle)	Paclitaxel	Breast cancer, Japan	Clinical Phase III
		Gastric cancer, Japan	Clinical Phase II
		Solid tumours, Japan	Clinical Phase I
SP1049C (Micellar doxorubicin – pluronic F127:L61 (1:8)	Doxorubicin	Gastric cancer; Oesophageal cancer	Clinical Phase II/III (FDA orphan drug status - 2007)
EndoTAG-I/lipopack	Paclitaxel	Triple negative breast cancer and pancreactic cancer (mutual with gemcitabine)	Clinical Phase II (FDA Orphan drug status, 2006)
Atragen (Liposomal all trans-retinoic acid)	Tretinoin	APM	Clinical Phase II
Aurimmune/CYT-6091 (colloidal gold-bound tumor necrosis factor)	TNF	NSCLC	Clinical Phase II
BIND-014	Docetaxel	Squamous histology NSCLC and cervical, head and neck cancers	Clinical Phase II
MBP-426 (Lipossomal oxaliplatin)	Oxaliplatin	Metastatic gastric, gastro-esophageal junction or esophageal adenocarcinoma	Clinical Phase II
MM-302 (HER2- targeted pegylated liposomal doxorubicin)	Doxorubicin	Metastatic breast cancer	Clinical Phase II
Aroplatin (NDDP liposome)	NDDP, cisplatin analog	Metastatic CRC	Clinical Phase II
CRLX101 (Camptothecin-cyclodextrin-polyethylene glycol copolymer)	Camptothecin	Relapsed ovarian cancer (plus placitaxel or bevacizumab)	Clinical Phase I/II (FDA Orphan drug status, 2015)
		Metastatic renal cell carcinoma (combined with bevacizumab)	Clinical Phase II (FDA Fast Track designation)

Table 2.2 (continued)

Nanoparticulate system	Drug/Active ingredient	Potential application	Phase Trial
LEP-ETU/NeoLipid (Paclitaxel liposome)	Paclitaxel	Metastatic breast cancer	Clinical Phase II
		Ovarian cancer	Clinical Phase I (FDA Orphan Drug Status, 2015)
NK012/SN-38 nanopolymeric micelle	Irinotecan SN-38 (Irinotecan ative metabolite)	Breast cancer; CRC; Multiple myeloma; Small cell lung cancer	Clinical Phase II
		Solid tumours	Clinical Phase I
CRLX301	Docetaxel	Advanced solid tumors	Clinical Phase II
SGT53 (Transferrin receptor-Liposome-p53 Complex)	p53-gene	Glioblastoma; Pancreatic cancer	Clinical Phase II
		Solid tumours	Clinical Phase I
Liposomal annamycin	Annamycin	ALL	Clinical Phase I/II
ProLindac(DACH-Pt polymer)	DACH-Pt	Ovarian Cancer	Clinical Phase I/II
Atu027 (Liposomal RNA interference)	siRNA	Pancreatic cancer	Clinical Phase I/II
		Solid tumours	Clinical Phase I
Alocrest (Optisomal Vinorelbine tartrate)	Vinorelbine	Breast cancer and NSCLC	Clinical Phase I
Brakiva (Optissomal topotecan hydrochloride)	Topotecan	NSCLC, Myelodysplastic Syndromes, Ovarian Cancer and AML	Clinical Phase I
CALAA-01 (cyclodextrin polymer-based nanoparticles)	siRNA	Relapsed or refractory cancer	Clinical Phase I
Docetaxel- polymeric nanoparticle	Taxane docetaxel	Advanced Solid Tumors	Clinical Phase I
NK911 (Micellar doxorubicin)	Doxorubicin	Solid Tumors	Clinical Phase I (Japan)
NC-4016 (1,2- DACH-Pt-polymeric micelles)	DACH-Pt	Solid Tumors	Clinical Phase I
S-CKD602 (Pegylated liposomal CKD-602)	Belotecan (CKD 602)	Refractory solid tumors	Clinical Phase I
SGT 94 (Transferrin receptor - Lipossomal RB94 plasmid)	RB94 plasmid DNA	Solid Tumors	Clinical Phase I
Lipovaxin MM (Multi-component liposomal nanoparticle-based)	Melanoma antigens and IFNγ	Malignant melanoma	Clinical Phase I (Australia)
C-VISA-BikDD liposome (DOTAP:cholesterol)	Plasmid C-VISA BiKDD	Pancreatic cancer	Clinical Phase I
C225-ILS-DOX (Doxorubicin anti-EGFR immunoliposomes)	Doxorubicin	Solid tumours	Clinical Phase I

Abbreviations/Acronyms: FDA, Food and Drug Administration; EMA, European Medicines Agency; RCW, Recurrent chest wall; HIFU, high intensity focused ultrasound; HER, Receptor tyrosine-protein kinase erbB-2; NDDP, Cis-bisneodecanoato-trans-R,R-1,2-diaminocyclohexane platinum II; DACH-Pt, diaminocyclohexane platinum; NSCLC, non-small cell lung cancer; CRC, colorectal cancer; ALM, acute myeloid leukemia; ALL, acute lymphocytic leukemia; APM, Acute promyelocytic leukemia; IFNγ, interferon gamma

References: Hafner et al., 2014; Hang et al., 2016; Jin et al., 2014; Pillai, 2014; Raju et al., 2015; Sanna et al., 2014; Ventola, 2012 and the corresponding and supplementing sources (FDA, EMA and pharmaceutical companies' websites)

2.4. The role of polymeric nanoparticles in nanotheragnostic development

…size and composition as favourable contribution.

Regarding biological applications, it is important to manipulate nanotechnology focusing on the primary needs of biosystems: biocompatibility, bioavailability and biodegradability. The combination of these properties allows acceptance by the biological system, delivery and effective action, active elimination of the systems and aims to prevent toxicity and immunogenic responses. Towards this purpose, polymers are a potential option, being widely applied as biomaterials in engineering, pharmacological and clinical developments (Marin et al., 2013). Polymeric chains consist on repeated simple and small units, whose arrangement and composition defines its physicochemical properties. This versatility allow to design and modulate systems to specific and diverse applications. The final properties required for a certain purpose, type of action and administration pathway, are possible to be optimized according to the type of formulation and by combination with other compounds.

Despite the interest and potential of polymer-based nanoparticles, currently there are no approved therapies based on these systems for clinical application. However, there is a great focus on its development, as its shown by the ongoing clinical trials (Table 2.2).

2.5. mPEG-co-PCL nanoparticles by nanoprecipiation

…simple is better.

Methoxy polyethylene glycol-co-poly ε-caprolactone (mPEG-co-PCL) is an amphiphilic diblock copolymer resulting from ring-opening polymerization synthesis (Figure 2.1). In the field of nanotechnology, is described as a biocompatible and biodegradable drug delivery system with advantageous properties regarding sustained and controlled release.

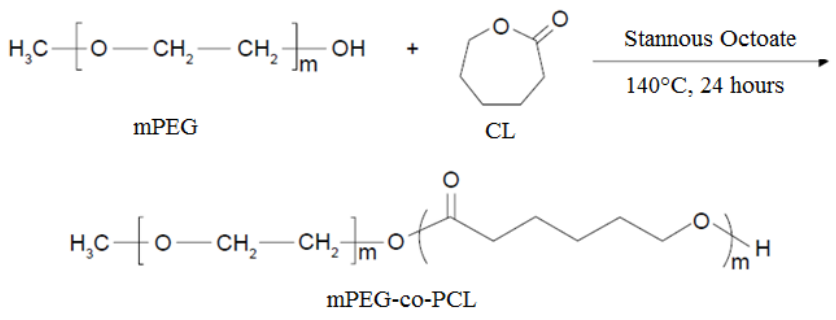

Figure 2.1 - Schematic representation of methoxy polyethylene glycol (mPEG) and ε-caprolactone (CL) copolymerization, to form copolymer mPEG-co-PCL, adapted from Xiong et al., 2015.

The mPEG-co-PCL nanoparticles present spherical shape, small sizes (from 100 to 140 nm) and uniform monodispersity, which contributes to a prolonged blood circulation time, enhances the

accumulation in tumours and endocytic uptake and prevents rapid elimination by the reticuloendothelial system (RES) (Baimark & Srisuwan, 2012; Baimark, 2009; Danafar & Schumacher, 2016; Xiong et al., 2015). This nanosystems design is based on 'synergetic' combination of both poly ε-caprolactone (PCL) and methoxy polyethylene glycol (mPEG) in order to integrate the favourable properties of the two polymers in a unique system, bypassing their individual disadvantages. PCL is commonly designed as drug carrier due to its biocompatibility, non-cytotoxicity, high solubility, low glass transition temperature (T_g) and high drug permeability, conferred by its hydrophobicity. However this hydrophobic character and its semi-crystalline structure enhance its susceptibility to RES clearance and confer low degradation rates, respectively. The copolymerization with mPEG allows to achieve a positive equilibrium in terms of biodegradability, RES clearance reduction and higher blood circulation periods, because of its hydrophilicity and flexibility (Danafar & Schumacher, 2016; Xiong et al., 2015). Besides, mPEG allows to functionalize nanoparticles surface without additional surface modifications and prevents nanoparticles agglomeration (Baimark & Srisuwan, 2012), avoiding the use of surfactants which enable to maintain the 'green' character of the synthesis procedure – nanoprecipitation.

Nanoprecipitation, also called solvent displacement method, is a one step procedure with easy and rapid reproduction, based on the polymers relative solubility in two miscible solvents. The standard procedure normally takes advantage of polymer solvation in a non-toxic organic solvent, where the drug and surfactants (optional) are also soluble, forming a homogenous solution. When dropped into an aqueous solution, in which the polymer is less soluble (non-solvent), the fast diffusion of the solvent causes polymer precipitation. This phenomenon is responsible for nanoparticles formation with simultaneous drug entrapment (Minost et al., 2012). Since it is a mild process, requiring low energy (Xiong et al., 2015), it can be considered a green approach, when applied without surfactant.

2.6. Chitosan

…discovered 200 years ago (Braconnot).

Chitosan is a natural cationic polysaccharide that results from partial chitin deacetylation originating random linear combinations of β-1,4-linked glucosamine and N-acetyl-D-glucosamine units. Its intrinsic properties are greatly influenced by the molecular weight, varying from 10 to 1,000 kDa, and deacetylation degree, normally in the range of 70-95% (Hamman, 2010). Given its high availability, low production cost and valuable properties regarding biocompatibility, biodegradability and low metabolic and immunogenic toxicity, it is repeatedly described in the literature as suitable delivery system in several different fields and applications. It is considered very promising regarding cancer because of its mucoadhesivity, tending to selective accumulate in mucous, preferentially in

anionic cancer cell surface due to its cationic nature. Other published characteristics are related with tumour growth suppression, immune system adjuvant and anti-inflammatory activity, which confer to this compound an anti-tumoral contribution (Pujana et al., 2013; Aruna et al., 2013; Park et al., 2010; Pujana et al., 2012). Besides, there are many benefits regarding other biomedical purposes – antifungal, antioxidant, anticholesterolemic, antimicrobial (Je & Kim, 2012)

Two major drawbacks in chitosan bio applications are its low solubility at physiologic pH (≈7.4) and its fast dissolution in the stomach (Park et al., 2010; Pujana et al., 2012), both explained by chitosan pK_a (≈ 6.3-7) (Pujana et al., 2012). At pH above pK_a, the non-protonated amino groups form strong hydrogen interactions within the chain, limiting external interactions and its solubility state. At acidic pH (below pK_a), the weakening of inter-chain interactions due to amino protonation leads to chitosan dissolution. This behaviour can be controlled by using derivatives or combined systems. Moreover, this chitosan pH sensibility can be an advantage in terms of loading and strategic delivery,, for instance, to prevent drug release at physiologic pH, promoting its preferential release in tumour acidic environment or lisossomes or endossomes, in the case of internalization (Arteche Pujana et al., 2014) .

2.6.1. Chitosan-based nanosystems for colorectal cancer

The use of chitosan-based nanocarriers for pharmaceutical purposes leads to bioavailability enhancement and greater drug absorption and retention time (Aruna et al., 2013; Cerchiara et al., 2015). Concerning cancer delivery, there are a lot of published applications to generic tumour cells (Lee et al., 2014; Mehrotra, Nagarwal, & Pandit, 2011; K. Park et al., 2007; Yoon et al., 2014) and specific cancers as lung (Maya et al., 2014), liver (Guan et al., 2012; Qi, Xu, & Chen, 2007; Zhu et al., 2013), breast (Deng et al., 2014), brain (Veiseh et al., 2010), colon (Feng et al., 2015) and others. Several studies in this field have been done for colorectal cancer tissues aiming at diagnosis and therapeutics. In 2008, Yang, Chen, & Shieh reported *in vivo* promising results for a chitosan-folic acid conjugated system, carrying a contrast dye (*indigo carmine*) for endoscopic detection of colorectal cancer cells. Similar approaches referred chitosan nanoparticles and chitosan-folic acid nano-conjugates as adequate carriers for oral administration of 5-aminolaevulinic acid (5-ALA), as fluorescent compound for colorectal cancer diagnosis. Those systems were developed with a perspective of further improvement, in order to reduce chitosan dissolution in the stomach (S. J. Yang et al., 2010; S.-J. Yang et al., 2009). Venkatesan et al presented, in 2011, promising outcomes from mouse human xenograph models for the use of a hydroxyapatite-chitosan nanosystem as transporter and delivery-agent for celecoxib and other drugs, aiming colon cancer treatment. In 2012, Xu et al published potential results for a chitosan-based nanosystem, modified with tripolyphosphate (TPP) to deliver interleukin-12 (IL-12). Focusing on the prevention of colorectal cancer liver metastasis, the

tests were made *in vivo* in mouse models, revealing an effective promotion of liver antitumor immunity. Another study, presented by Khatik et al (2013), refers the advantages of using Eudragit S 100-coated chitosan nanoparticles (ES-CS-NPs) loaded with curcumin in comparison to chitosan nanoparticles, for colon cancer treatment. The ES-coating showed benefits regarding targeted release and the results suggest that ES-CS-NPs are more biocompatible. In turn, Malhotra et al (2013) studied pegylated chitosan nanoparticles tagged with CP15 peptide to target colon cancer cells, for therapeutic gene delivery of PLK1-siRNA. The *in vivo* experiments using this formulation in mouse xenograft model of colorectal cancer, showed promising results as non-invasive application for gene therapy. An *in vivo* investigation of the combined effect of 5-fluorouracil (5-Fu) and curcumin for the treatment of colon cancer, demonstrated that the individual encapsulation in thiolated chitosan nanocarriers improves drugs bioavailability and enhances their anticancer effect, when compared to non-encapsulated combined drugs (Anitha et al., 2014). Feng et al (2015) produced a promising alternative for colorectal cancer therapy based on mucoadhesion improvement by using chitosan-carboxymethyl-chitosan-$CaCl_2$ (CS-CMCS-Ca^{2+}) nanoparticles loaded with doxorubicin hydrochloride (DOX). A recent investigation (Ravikumar et al., 2016) resulted in the preliminary development and characterization of chitosan-hydroxy ethyl cellulose-poly vinyl alcohol, as suitable and useful nanofibers for 5-Fu-controlled release against colorectal cancer.

These developments are summarized in Table 2.3.

Table 2.3 – List of chitosan-based nanoparticles, in development for colorectal cancer.

Nanoparticulate system	Functionalization	Application	Author/Year
Chitosan-folic acid	-	Diagnostic: indigo carmine detection	Yang et al., 2008
Chitosan	-	Diagnostic: 5-aminolaevulinic acid delivery	Yang et al., 2009
Chitosan-folic acid	-	Diagnostic: 5-aminolaevulinic acid delivery	Yang et al., 2010
Chitosan - tripolyphosphate	-	Prevention: interleukin-2 delivery	Xu et al., 2012
Eudragit S 100-coated chitosan	-	Targeted therapy: curcumin delivery	Khatik et al., 2013
Chitosan-PEG-CP15peptide	PEG-CP15peptide	Therapy:Biotin-siRNA delivery	Malhotra et al., 2013
Thiolated-chitosan	-	Therapy: combined delivery of curcumin and 5-fluorouracil (loaded independently)	Anitha et al., 2014
Chitosan-carboxymethyl-chitosan-$CaCl_2$	-	Therapy: delivery of doxorubicin hydrochloride	Feng et al., 2015
Chitosan-Hydroxy Ethyl Cellulose-Poly Vinyl Alcohol	-	Therapy: 5-fluorouracil delivery	Ravikumar et al., 2016

Abbreviation: PEG, polyethylene glycol

2.7. Collagenase application in nanotechnology

Collagenase is a proteolitic enzyme responsible for the digestion of native collagen. The degradation of collagen, an important component of the extracellular matrix, helps to bypass the penetration limitations imposed by that conjunctive barrier (Goodman, Olive, & Pun, 2007; Murty et al., 2014). Therefore, collagenase has been studied for anticancer nanomedicine or nanopharmaceutical applications, as active contributor in terms of achieving a deeper tumoral penetration and consequently, higher efficiency in nanoparticles accumulation and action.

Goodman, Olive, & Pun published in 2007 the first study corroborating collagenase advantages for this purpose. The results obtained revealed a four-fold enhancement of spheroids core penetration by collagenase-coated polystyrene nanoparticles in comparison to the control albumin-coated nanoparticles. Another group showed that the pre-intravenous administration of collagenase in mice bearing mouse Lewis lung carcinoma, for further lipoplex delivery, increased tumour accumulation 1.5-fold and amplified the gene expression 2-fold (Kato et al., 2012). Moreover, in 2014, Murty et al., described nanoparticles functionalization with collagenase as a promising pathway to increase accumulation within tumours, based on tests of collagenase-pegylated gold nanoparticles in mice tumour xenografts, demonstrating an improvement of 35% in core accumulation, comparing to non-functionalized nanoparticles.

Recently, Villegas, Baeza, & Vallet-Regí (2015) presented an alternative and more complex model, for surface-transport of collagenase, aiming to avoid its exposure to blood circulating agents, as proteases. In this model, the authors attached pH-responsive polymeric-nanocapsules containing collagenase to the surface of mesoporous silica nanoparticles, to trigger collagenase release only in acidic conditions, similar to tumoral pH. Studies in three-dimensional models of human osteosarcoma cells showed considerable enhancement of tumours inner penetration.

The investigations did not report toxic effects of collagenase in human cells, being considered a safe additive for further developments.

The present work suggests a novel form of collagenase incorporation in the nanoparticulate systems and a new application for collagenase regarding colorectal cancer, as detailed below.

2.8. Chitosan-collagenase nanoparticles by inverse microemulsion

Moilanen et al. published results in 2015 that corroborate the title of their publication, ‘Collagen XVII expression correlates with the invasion and metastasis of colorectal cancer’. The authors revealed an unexpected collagen expression in colon epithelia and its overexpression in colorectal cancer. The study suggests an overexpression enhancement in metastatic stages.

Based on this, we postulated the use of collagen as a biomarker for metastatic colorectal cancer and we have designed a nano-delivery system incorporating collagenase as collagen recognizer, that would contribute for a preferential accumulation of nanoparticles in metastasis of colorectal cancer.

The collagenase incorporation was projected to occur through a genipin-based crosslink reaction, adapted from a chitosan-based nanospheres protocol (Pujana et al., 2013). This was possible due to the chemical groups involved in the reaction. As shown in Figure 2.2, the chitosan nanoparticles are synthesized by covalent crosslink between chitosan amine groups and the ester and dihydropyran ring of genipin. Since collagenase is also composed by amine groups, it can be crosslinked with genipin. Assuming collagenase integration as a chitosan-equivalent polymer in the synthesis procedure, simultaneous crosslink of both polymers is expected to occur, with no predefined order, forming chitosan-collagenase nanogels.

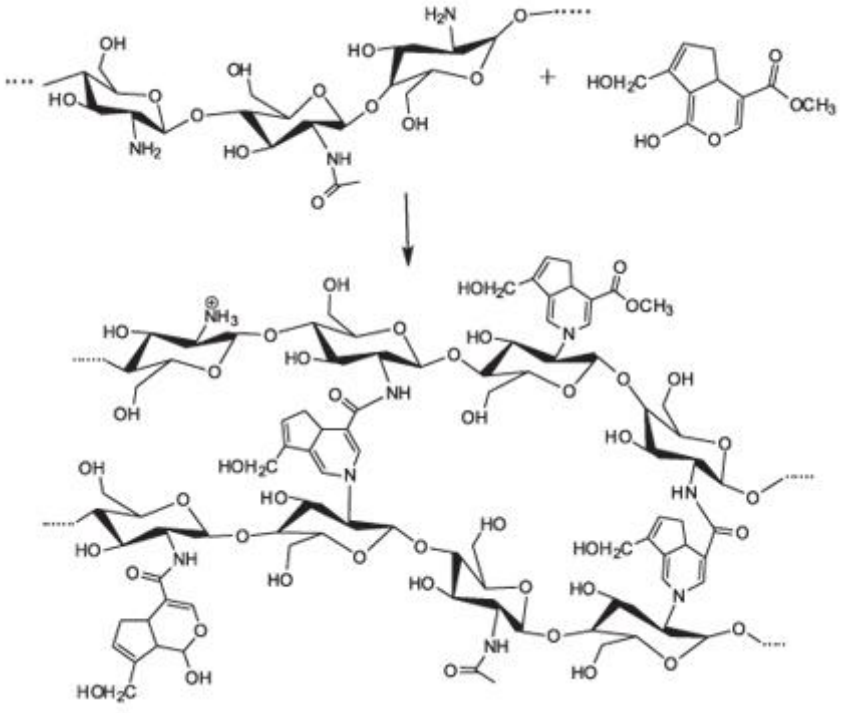

Figure 2.2 - Schematic representation of crosslink between chitosan (left) and genipin (right), from Lins et al., 2014.

The hybrid polymeric nanoparticles of chitosan and collagenase are expected to be biocompatible, bioavailable and biodegradable systems, combining the favourable properties of each polymer regarding specificity and efficiency of the delivery. Concerning nanoparticles accumulation, the use of collagen as biomarker allows to target colorectal cancer metastasis, with tumoral stronger adhesion and preferential accumulation conferred by chitosan mucoadhesivity and cationic nature. Besides, the enzymatic degradation of the extracellular tumour matrix allows the nanoparticulate

systems to reach the inner core, enhancing the therapeutic efficiency, also selectively directed to tumoral environment by using chitosan pH-sensitivity to trigger the drug release only in acidic environments, characteristic of tumoral surrounding.

The synthesis method reproduced, inverse microemulsion, also known as water–in-oil (W/O) microemulsion, is based on a thermodynamic equilibrium of water, oil and surfactant phases, in which the water amount is comparatively low, forming nanometric and monodisperse reverse micelles, with a polar inner core, containing polar or ionic compounds. The constant dynamic motion in solution - Brownian motion - leads to micelle collisions and fusion-fission occurrences, involving exchange and mixing of contents. The contact between reactants within micelles, forms 'nanoreactors', initiating the nanoparticles synthesis reaction by nucleation and controlled growth, limited and stabilized by the surfactant layer (Malik, Wani, & Hashim, 2012).

3. EXPERIMENTAL SECTION

3.1. Materials

Methoxy poly(ethylene glycol) (mPEG, molecular weight Mn = 5,000 Da, Aldrich, Germany), ε-caprolactone (CL) monomer (97%, Sigma-Aldrich, USA), Stannous octoate ($Sn(Oct)_2$; 92,5-100%, Sigma, Japan), phenethyl isothiocyanate (PEITC, 99%, Aldrich, USA), coumarin-6 (C6, Santa Cruz Biotechnology, Dallas), chitosan (low molecular weight, Aldrich, USA), collagenase type I (Gibco Life Technologies, USA), genipin (98%, Wako chemicals, Germany). All solvents used were of analytical grade.

3.2. Synthesis and characterization of block copolymer mPEG-co-PCL

The methoxy polyethylene glycol-co-poly ε-caprolactone (mPEG-co-PCL) was synthesized by ring opening polymerization, adapted and optimized from Baimark, 2009; Baimark & Srisuwan, 2012; Xiong et al., 2015. The final synthesis was made as follows:

9.4 g of ε-CL (≈ 80 mmol), 2.2 g of mPEG (≈1 mmol) and 3.4 g of $Sn(Oct)_2$ (≈ 0.1 mol% of monomer ε-CL) were added into a glass tube and submitted to a vacuum system under nitrogen refilling for about 2 hours. The tube was kept sealed and heated to ≈140°C in an oil bath for ≈24 h. The mixture was cooled to room temperature and dissolved in dichloromethane. The product was precipitated and washed in cold n-hexane or diethylether. After total evaporation of the precipitant, the final product was dried at ≈ 35°C, in an incubator. The copolymer structure was confirmed by ^1H – NMR (nuclear magnetic resonance) in a Bruker Avance III 400MHz, Fallanden equipment, using $CDCl_3$ as solvent. This protocol was optimized and requires further optimization to obtain a purer copolymer.

3.3. Synthesis of mPEG-co-PCL nanoparticles

mPEG-co-PCL nanoparticles (NPs) were produced by nanoprecipitation, adapted and optimized from Baimark, 2009; Baimark & Srisuwan, 2012; Xiong et al., 2015.

10 mL of solvent were added to 10 mg of drug/marker and 100 mg of mPEG-co-PCL and submitted to vortex and sonification. The mixture was added dropwise to 100 mL of miliQ H_2O, under stirring. The suspension was stirred overnight to remove the solvent and centrifuged to 15 000 rpm, 4°C during 60 minutes. The pellet was lyophilized during 42h.

Based on the cited procedures, the solvent used for both empty and C6-loaded NPs was acetone. For the loading of PEITC, a mixture of acetone:etanol (1:1) was used, taking into account the solubility properties of the copolymer and PEITC.

3.4. Characterization of mPEG-co-PCL nanoparticles

The particles size was analysed by Dynamic Light Scattering (DLS) equipment (Zetasizer Nano Series, Malvern Instruments Ltd, UK). The samples for the analysis were dissolved in filtered bidistilled water and submitted to sonication and pre-equilibration at 25°C.

Field Emission Gun Scanning Electron Microscopy (FEG-SEM) (JEOL, model JSM7001, Japan) was also used to examine particle size and morphology. The samples were prepared for observation by covering with gold/palladium (Au/Pd), in a sputter coater (Quorum Technologies, model Q150TES). Micrographs of the prepared aliquots were taken at an acceleration voltage of 15kV.

3.5. Synthesis of chitosan and chitosan-collagenase nanoparticles

The chitosan-genipin NPs were produced by inverse microemulsion, adapted from Pujana *et al* (2013). This synthesis was made to confirm the reproducibility of the procedure and as control, since it was applied for the development of the new system, chitosan-collagenase.

Two different microemulsions were prepared. To the first one, chitosan was prepared in 1% (v/v) aqueous acetic acid solution to a concentration of 10 mg/mL A mixture of cyclohexane:*n*-hexanol:chitosan was prepared to a final ratio of 2.75:1:1. Triton X-100 was added dropwise until the solution became transparent. The second microemulsion was prepared by adding genipin in excess (100 mg per mL of miliQ H_2O) to a mixture of cyclohexane:*n*-hexanol:miliQH_2O (2.75:1:1). This microemulsion was added to the first one, under stirring. After 7 days of crosslinking reaction, at room temperature, the solution was added dropwise to excess ethanol.

The chitosan-genipin-collagenase NPs were produced by reverse microemulsion, adapted and optimized from the work of Pujana and collaborators (Arteche Pujana et al., 2013).

Two different microemulsions were prepared. To the first one, chitosan was prepared in 1% (v/v) aqueous acetic acid solution to a concentration of 10 mg/mL and mixed with collagenase dissolved in miliQ H_2O, to a final ratio of 1:1. A mixture of cyclohexane:*n*-hexanol:chitosan-collagenase were prepared to a final ratio of 2,75:1:1. Triton X-100 was added dropwise until the solution became transparent. The second microemulsion was prepared by adding genipin to a mixture of cyclohexane:*n*-hexanol:miliQH_2O (2.75:1:1). The amounts of genipin were adapted to final ratios of 10:1; 2:5; 1:5 and 1:10 (genipin:chitosan-collagenase). This microemulsion was added to the first one,

under stirring. After 7 days of crosslinking reaction, at room temperature, the solution was added dropwise to excess ethanol.

3.5.1. Isolation and drying of chitosan and chitosan-collagenase nanoparticles

Several approaches were tested for obtaining dry and solvent/surfactant-free nanoparticles.

The first methodology tested was lyophilisation. The NPs were previously washed by several cycles of centrifugation at 8000 rpm for 15 minutes and ressuspension in ethanol. The final pellet was ressuspended in miliQ H_2O, frozen in liquid nitrogen and dried by lyophilisation (72 hours, FreeZone Plus 4.5 Liter Cascade Freeze Dry System**,** Labconco).

The second approach resorted to rotary evaporator/rotavap equipment (Rotavapor R-210, Butchi, Switzerland) at 37°C, coupled to a vacuum controller (V-850, Butchi, Switzerland) and subsequent wash with diethyl ether to remove the surfactant and remaining impurities.

A third method aiming for a one-step procedure was tested using an adsorbent membrane (NADIR UP-10) coupled to a vacuum controller (V-850, Butchi, Switzerland).

The last procedure applied was NPs washing by several cycles of centrifugation at 8000 rpm for 15 minutes and ressuspension in ethanol. The final pellet was further washed by agitation in diethylether to remove remaining impurities and vestigial solvents or surfactant.

3.5.2. Characterization of chitosan and chitosan-collagenase NPs

The nanoparticles size and morphology was studied recurring to FEG-SEM (JEOL, model JSM7001, Japan). The samples were prepared for observation by covering with gold/palladium (Au/Pd), in a sputter coater (Quorum Technologies, model Q150TES). Micrographs of the prepared aliquots were taken at an acceleration voltage of 15kV.

3.5.3. 5-Fluorouracil loading into chitosan and chitosan-collagenase nanoparticles

The following procedure was designed and optimized from Arteche Pujana et al., 2014**.**

Nanoparticles were suspended in a phosphate buffered saline (PBS) solution of 5´-fluorouracil (5´-Fu) at 20 or 40 ppm, according to a final NPs concentration of 1 or 3 mg/mL, respectively. These suspensions, prepared at pH 3 and 5.5 were stirred for at least 3h, for drug entrapment by swelling of the NPs network. Then, the pH was increased to values around physiologic pH (7.4) by adding NaOH and stirred during 1h, to diminish network swelling, avoiding drug liberation. The samples were centrifuged at 6000 rpm for 20 minutes and the supernatants collected and analysed by spectrophotometry at 264 nm to determine the encapsulation efficiency. To remove superficial drug, the nanoparticles were washed with PBS pH 7.4.

3.5.4. 5-Fluorouracil *in vitro* release

The release occurred by submitting the load nanoparticles to acidic PBS solutions (pH 3 and 5.5), under agitation during at least 3h. The samples were centrifuged at 6000 rpm for 20 minutes. The amount of 5-Fu in the supernatants was determined at 264 nm, by Beer-Lambert law. Calibration curves were previously prepared for 5-Fu quantification. The samples were prepared by successive dilution of a 100 ppm stock solution for final concentration of 80, 50, 20, 10, 5, 3, 2 and 1 ppm. The stock solutions and dilutions were performed using PBS at pH 3, 5.5 and 7.4.

4. RESULTS AND DISCUSSION

4.1. Block copolymer mPEG-co-PCL

The final yield of the copolymer synthesis was calculated by the formula:

$$\%\ \text{yield} = \frac{\text{Final weight}}{\text{Initial weight}} \cdot 100$$

The final weight corresponds to the mass of the powder obtained after synthesis and precipitation. The initial weight corresponds to the sum of the measured masses of the reagents involved in the synthetic procedure (ε-CL and mPEG).

During the optimization phases, the final yield was increased from 12 to 88%. It is expected to be enhanced in further stages of optimization.

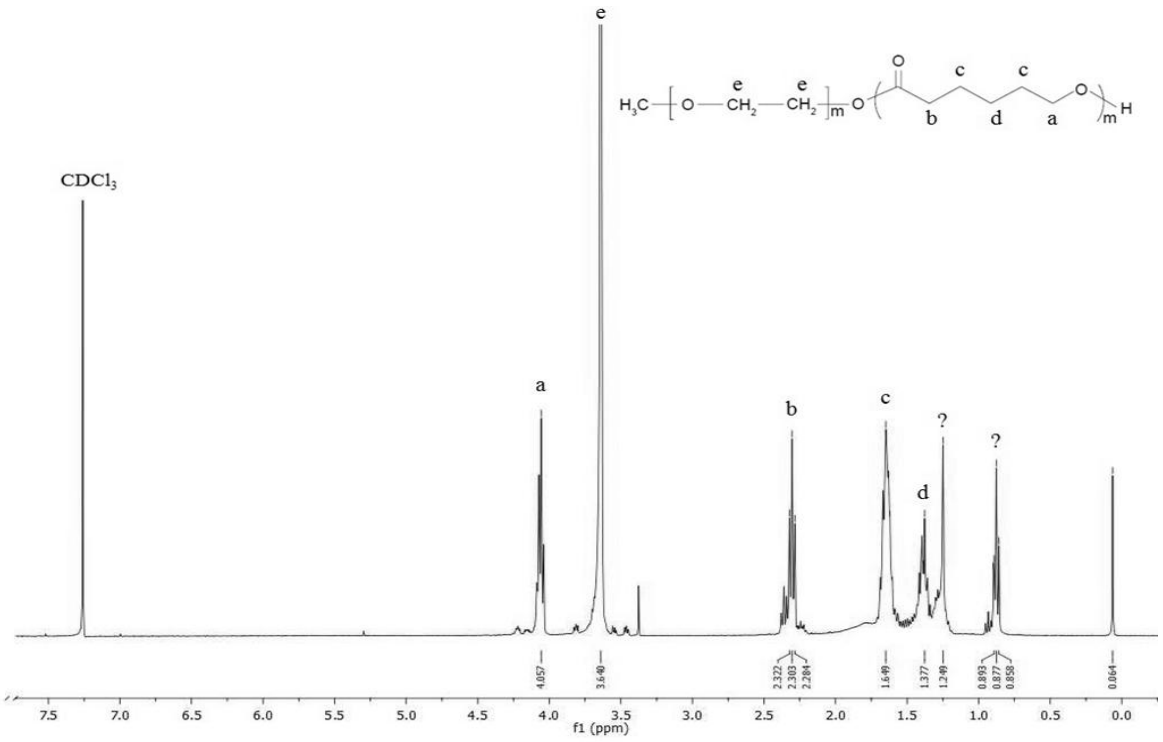

Figure 4.1 – ^{1}H-NMR spectrum obtained for chemical characterization of mPEG-co-PCL, obtained by a preliminary synthesis, similar to procedure described (data supported by literature published spectra - Figure 8.1, in appendix.)

During the polymer precipitation, it was noticed that the solution became yellow, which is a possible indicator of ε-caprolactone presence (specification sheet – Sigma Aldrich), probably resulting from an incomplete reaction. This supposition was confirmed by the NMR spectrum obtained from the precipitated powder (Figure 4.1). The δ = 1,249 ppm is not associated to any chemical group of mPEG-co-PCL. Analysing the individual components and intermediary forms involved in the

copolymerization, it was noticed that it may correspond to the isopropyl end group of poly(ε-caprolactone), since it has a similar chemical shift (Long et al., 2010, Figure 8.2-b). Despite being a confirmation of the initiation of ring opening polymerization (Figure 8.2-a), the presence of PCL also evidences the existence of intermediary compounds resultant from incomplete copolymerization between mPEG and PCL.

The other unexpected signal (δ ≈ 0,9ppm), is a triplet characteristic of methyl groups, which can result from the solvents used to precipitate the polymer, n-hexane or diethylether.

In addition, it is possible to observe interferences in the signals that confirm the existence of impurities in the product obtained by copolymerization. Therefore, the procedure was optimized until a higher degree of purity was achieved. The protocol described in the experimental section allowed to obtain the purest copolymer - Figure 4.2. By comparative analysis with published NMR spectra (Figure 8.1 in Appendix), it was assumed that the synthesized copolymer had an acceptable purity for preliminary studies regarding nanoparticles formulations. However, it was not possible to fully eliminate the precipitant interference, as it is possible to see at δ ≈ 0,9 ppm. For further studies, namely cellular tests, it is crucial to ensure the obtention of highly pure copolymer, solvent-free, to guarantee the reliability for *in vitro* and *in vivo* applications.

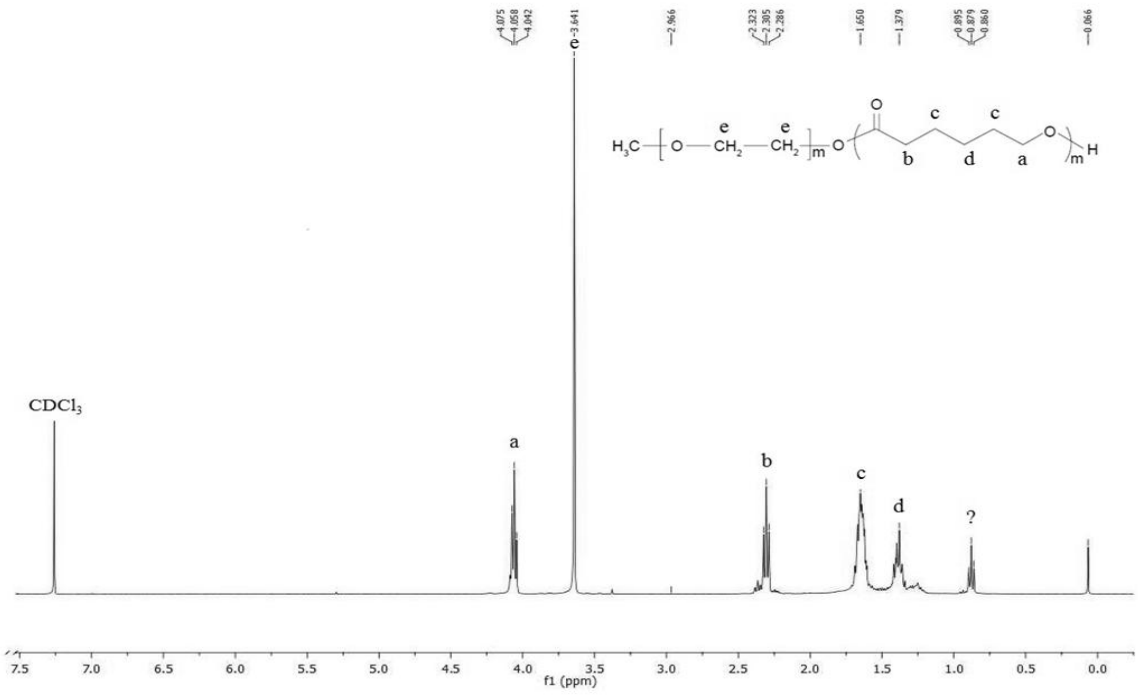

Figure 4.2 - ^{1}H-NMR spectrum obtained for chemical characterization of mPEG-co-CPL, synthesized by the described procedure (data supported by literature published spectra – Figure 8.1, in appendix.)

4.2. mPEG-co-PCL nanoparticles

Firstly, the protocol described above was performed, for obtaining empty nanoparticles, as control of the reproducibility.

The DLS analysis of the empty mPEG-co-PCL nanoparticles synthesized from a set of optimization stages, showed progression in terms of polydispersion decrease - Table 4.1.

Table 4.1 - DLS results obtained for empty mPEG-co-PCL nanoparticles, in different stages of optimization, ordered by progression (ascending from 1 to 3).

		Size (nm)			PdI range
		Maximum	Minimum	Median	
Progression stage	1	445	106	256	0.519 - 1
	2	295	144	209	0.342 - 0.522
	3	241	99	159	0.220 - 0.774

As indicated in the table, the maximum sizes measured by the DLS decreased during optimization, presenting median PdI values of 1, 0.402 and 0.386, for crescent optimization degrees, respectively. This PdI decrease resulted from less agglomerates in suspension and measurement of narrow size ranges, as clearly observed in Figure 4.3.

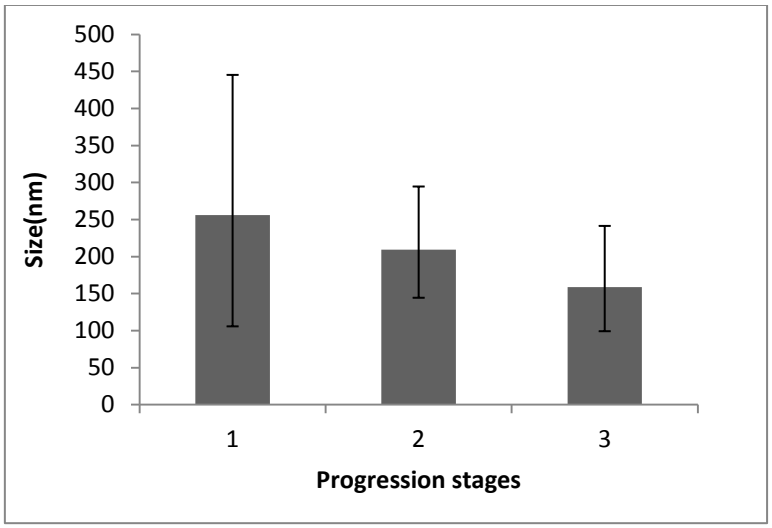

Figure 4.3 - Representation of size ranges obtained for the principal stages of optimization, ordered by progression (ascending from 1 to 3).

The measurements of initial optimization stages indicated the presence of significant amounts of agglomerates (sizes over 1000 nm), which can be due to interference of impurities or particles agglomeration, measured by the DLS equipment as a single 'body' - Figure 4.4.

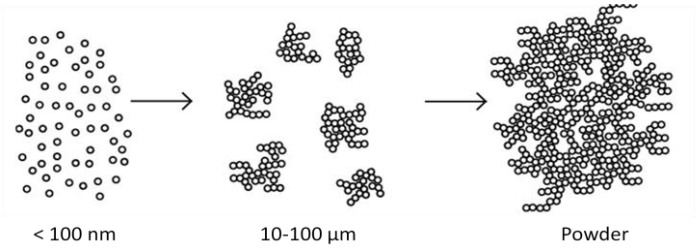

Figure 4.4 - Schematic representation of nanoparticles agglomeration, adapted from the online page of Product and Process Engineering - Delft University of Technology.

The agglomeration of particles can occur naturally due to chemical favourable stabilization or because of remaining compounds or solvents of the synthesis, that during the dry procedure, form a 'resin' that holds the nanoparticles as an unique structure. The occurrence of both phenomena was confirmed by observation of SEM images of the samples.

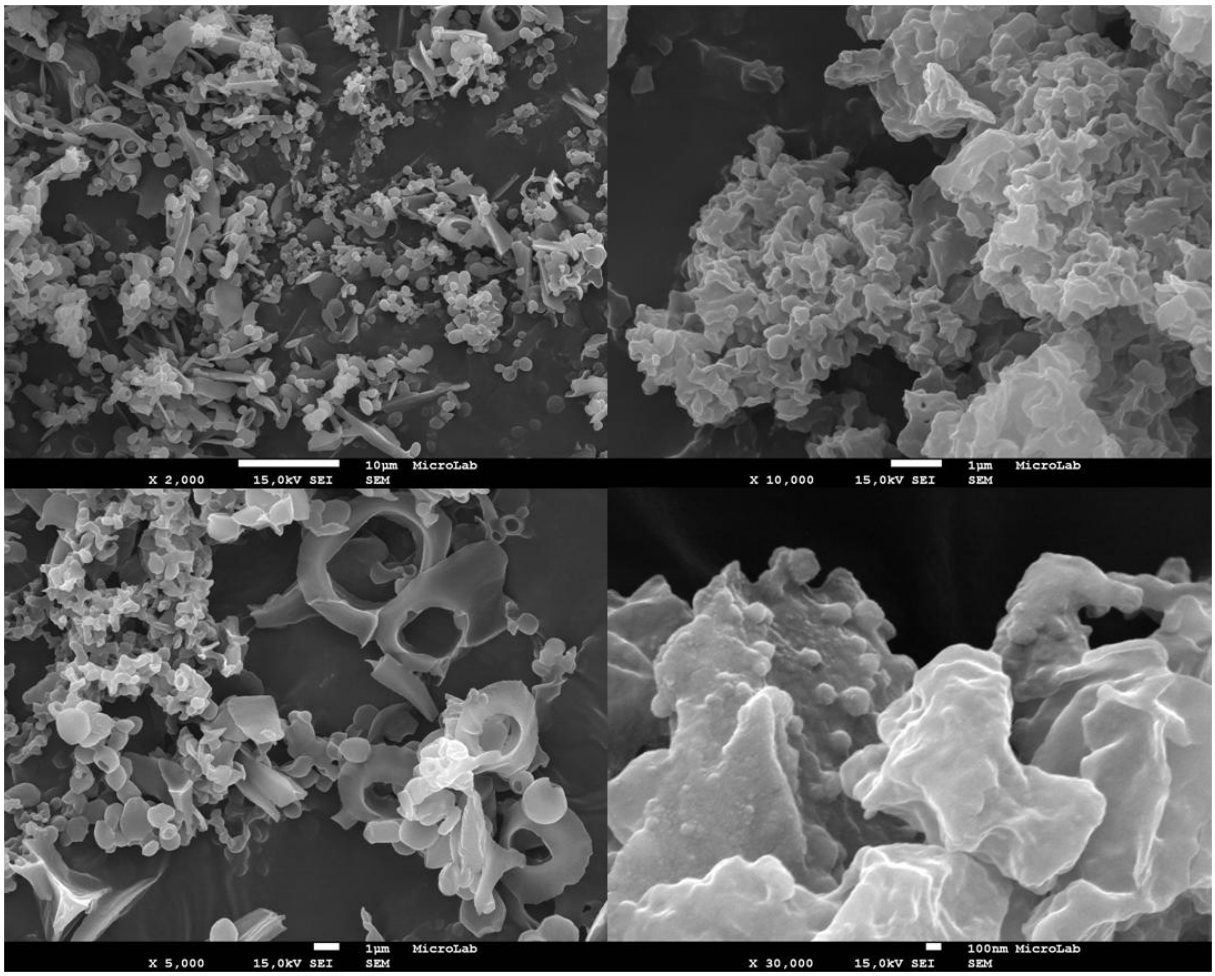

Figure 4.5 – FEG-SEM images obtained from samples obtained during optimization stages of mPEG-co-PCL nanoprecipitation. Left – Impurities (non spherical structures); Right – resin effect. (Scale bar: left top - 10 µm; left bottom - 1 µm; right top - 1 µm; right bottom - 100nm). .

In the left images contained on Figure 4.5, it is possible to observe non spherical structures that corroborate the existence of impurities, probably resulting from the copolymer powder. In the right images, it is visible the agglomeration of nanoparticles in a resin-like structure.

After a few stages of optimization, were obtained similar results to those reported in the literature, that describe an obtainment of spherical monodisperse nanoparticles, with published comparable sizes: less than 100 nm (Baimark, 2009), less than 140 nm (Baimark & Srisuwan, 2012), in the range of 120 to 140 nm (Xiong et al., 2015) and around 128 nm (Danafar & Schumacher, 2016). The data collected by these authors regarding size ranges and respective polydispersity, are summarized in Table 4.2.

Table 4.2 – Summarized information regarding size range and polydispersity of mPEG-co-PCL nanoparticles, according to the results published by the cited authors.

mPEG-co-PCL NPs size (nm)	**PdI**	**References**
]80 ; 100[	-	(Baimark, 2009)
]120 ; 140[	-	(Baimark & Srisuwan, 2012)
]120 ; 140[	0.121 - 0.136	(Xiong et al., 2015)
]120 ; 150[	0.166	(Danafar & Schumacher, 2016)

Notes: The '-' means that there is no available data regarding that parameter.
Abbreviations: mPEG-co-PCL NPs, methoxy polyethylene glycol-co-poly ε-caprolactone nanoparticles; PdI, polydispersity index.

The DLS results for the last mPEG-co-PCL NPs synthesis (Table 4.1 - progression stage 3) indicated measured sizes ranging from 99 to 241 nm, with a median size of 158 nm, near to the published ones - Table 4.2 - and a median polydispersity index of 0.385, significantly reliable for considering the sample as monodisperse. The higher size values probably correspond to agglomerates in suspension that interfere and compromise the reliability of DLS results.

To confirm the nanoparticles size and morphology, the sample obtained in the latest stage of optimization was analysed by FEG-SEM - Figure 4.6. As expected, the nanoparticles presented spherical shape and monodisperse sizes, around 100 nm.

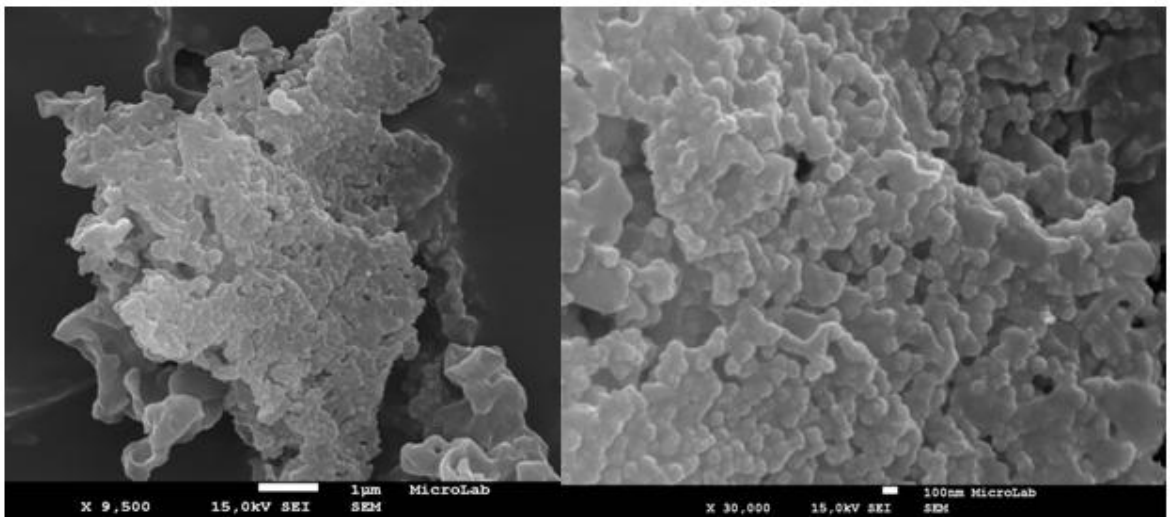

Figure 4.6 – FEG-SEM images of mPEG-co-PCL nanoparticles, synthesized in the latest stage of optimization (Scale bar: left - 1 µm; right - 100nm).

4.2.1. Loaded nanoparticles

In parallel to the synthesis of empty NPs, the production of coumarin-6 (C6)-loaded nanoparticles was reproduced and optimized from (Xiong et al., 2015), and used for the design of PEITC encapsulation. The loaded-NPs were first analysed by DLS, and compared to the empty nanoparticles, as schematically represented in Figure 4.7 and Figure 4.8.

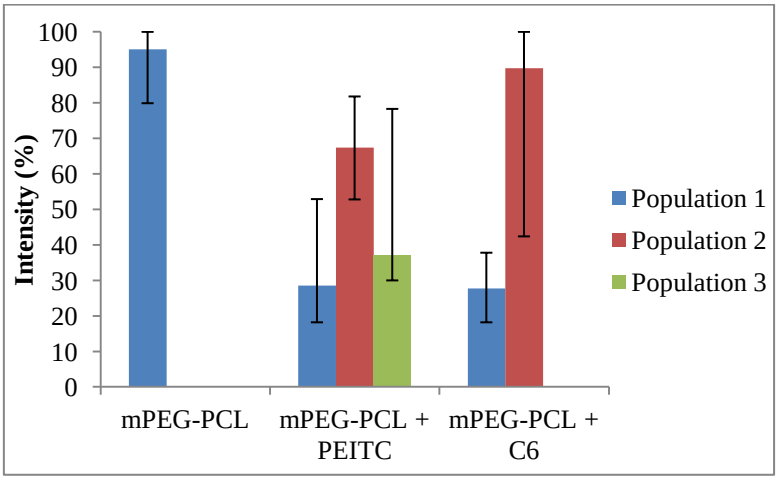

Figure 4.7 - Graphical representation of the intensity of each size range (population), obtained for empty and loaded mPEG-co-PCL NPs, indicating its median intensity (columns) and the respective variations (error bars). The population 1corresponds to the smallest size range and population 3 identify the larger ones.

The existence of more than one population size for the same nanoparticles sample is defined by the relative intensity measured for different sizes in suspension. If different sizes are identified in a significant percentage (>20%), they are considered individual population sizes, revealing a broad dispersity of nanoparticles.

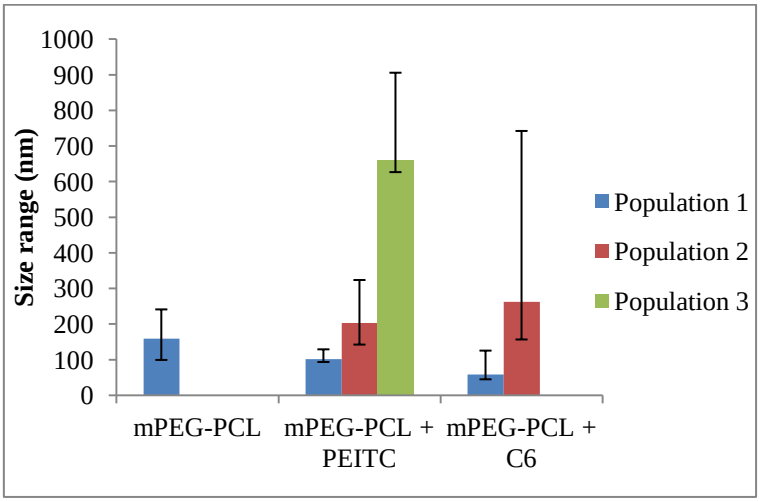

Figure 4.8 – Graphical representation of the population sizes obtained for empty and loaded mPEG-co-PCL NPs, indicating their median size (columns) and the respective variations (error bars).

As observed in the graphs of Figure 4.7 and Figure 4.8, three population sizes were identified for mPEG-co-PCL NPs loaded with PEITC and 2 population sizes for mPEG-co-PCL NPs loaded with C6, in comparison to the one population presented by the empty nanoparticles. This information and the remaining data collected from DLS measurements are summarized in Table 4.3

Table 4.3 - DLS results obtained for the loaded mPEG-co-PCL nanoparticles, in the first stages of synthesis in comparison the optimized results obtained for empty nanoparticles.

	Population	Size range (nm)	Median size (nm)	Intensity range (%)	PdI range	Agglomerates intensity range (%)
mPEG-PCL	1	]99;241[	159	80 - 100	0.220 - 0.774	0 - 20
mPEG-PCL + PEITC	1	]93;130[	102	18 - 53	0.332 - 1.000	0 - 10
	2	]142;324[	203	53 - 82		
	3	]626;906[	660	30 - 79		
mPEG-PCL + C6	1	]44;126[	59	18 - 38	0.467 - 1.000	0 - 23
	2	]156;743[	263	42 - 100		

Note: The agglomerates intensity range was considered for sizes above 1000 nm.

The DLS measurements for C6-loaded nanoparticles indicate a major incidence of sizes between 156 and 743 nm, presenting high polydispersity and a significant incidence of agglomerates. Since coumarin-6 is fluorescent, it interferes with the analysis, therefore, DLS methodology is not adequate to analyse this sample. The C6-loaded mPEG-co-PCL NPs was thus analysed by FEG-SEM, in order to obtain reliable results regarding size and morphology - Figure 4.9.

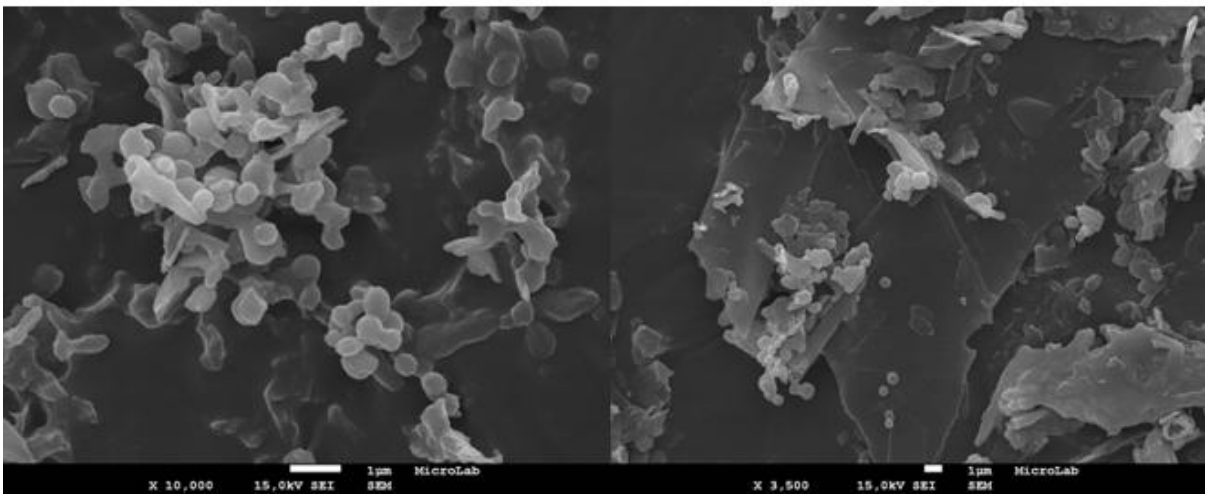

Figure 4.9 – FEG-SEM images obtained for coumarin-6-loaded mPEG-co-PCL nanoparticles (Scale bar: 1 µm).

As seen in the figure, there are spherical structures with sizes higher than 100 nm. However, the presence of non-defined structures is clear, problably corresponding to non-encapsulated coumarin or other impurities. This results suggests that the nanoprecipitation was not efficient. Since the encapsulation of C6 is already published by other authors but there is no significant description data available, the experimental studies were focused on the development of PEITC-loaded NPs, as a novelty concerning the mPEG-co-PCL nanoparticulate system.

The DLS measurements regarding PEITC-loaded nanoparticles (Table 4.3) indicate a main prevalence of sizes in the range of 142 to 324 nm, presenting also a high incidence of measured sizes above 626 nm, probably due to agglomeration.

In subsequent studies to test the stability of nanoparticles in suspension, the sample of mPEG-co-PCL loaded with PEITC was submitted to agitation to promote solvation, enhancing the monodispersity of the suspension. Additionally, the nanoparticles concentration in solution was also studied since it influences the agglomeration. By diluting the sample, it is expected to decrease the agglomeration phenomenon. Furthermore, the occurrence of sedimentation was studied by submitting the nanoparticles to several periods of rest. The sedimentation tends to increase the number of agglomerated structures.

These conditions were reproduced experimentally, in a standard sample with an initial concentration around 1 mg/mL. The effect of those conditions in size dispersion is exemplified in Figure 4.10, from data collected by DLS analysis. The remaining information is summarized in Table 4.4.

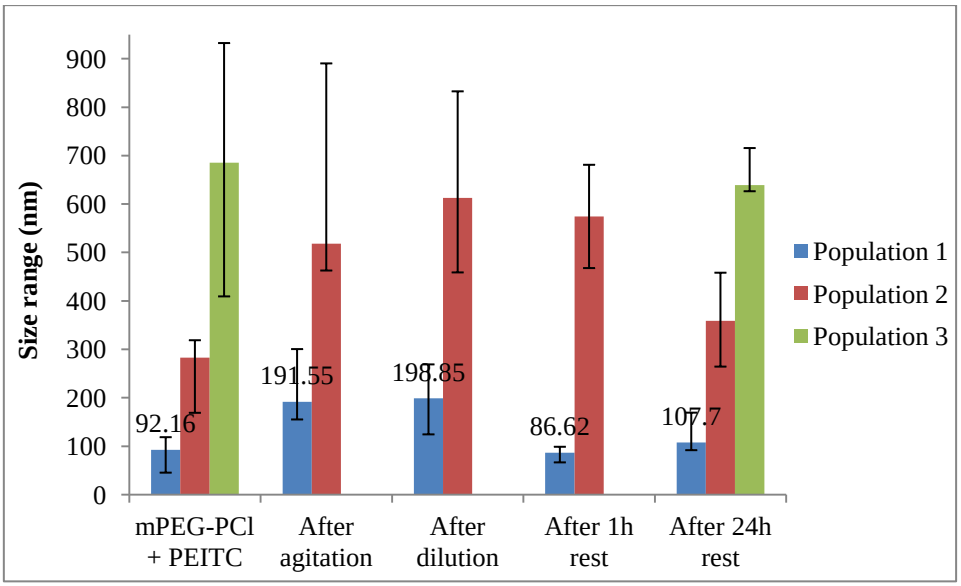

Figure 4.10 – Summary of the median sizes measured by DLS and its variations, before and after submitting a sample of mPEG-co-PCL loaded with PEITC to periods of agitation, dilution and subsequent rest.

After agitation, it was noticed the prevalence of intermediate and bigger sizes in comparison to the standard solution, confirming the existence of agglomerates in solution that 'mask' the smaller sizes. After dilution, the results remain similar to those obtained after agitation, in terms of sizes and intensities - Figure 4.10 and Table 4.4 – which can be due to insufficient time to reach a new equilibrium in solution. Another possibility is the interference of impurities or free drug in solution, further confirmed by the FEG-SEM images - Figure 4.11 and Figure 4.12.

Table 4.4 . DLS results obtained for the PEITC loaded mPEG-co-PCL nanoparticles, before and after submitting the sample to periods of agitation, dilution and subsequent rest.

	Population	Size (nm)	Median size (nm)	PdI range	Intensity range (%)
mPEG-PCL + PEITC	1	]45;119[	92	0.446 - 1.000	8 - 20
	2	]168;319[	283	0.574 - 0.953	42 - 100
	3	]409;933[	686	0.446 - 1.000	59 - 92
After agitation	1	]155;301[	192	0.583 - 0.977	15 - 36
	2	]462;891[	518	0.185 - 0.632	85 - 100
After dilution	1	]124;269[	199	0.743 - 0.909	7 - 50
	2	]458;833[	613	0.002 - 1.000	50 - 100
After 1h rest	1	]66;99[	87	0.303 - 0.606	5-6
	2	]467;681[	575	0.294 - 0.606	94-100
After 24h rest	1	]91;170[	108	0.295 - 0.526	8 - 36
	2	]264;459[	359	0.295 - 0.542	43 - 100
	3	]626;716[	639	0.410 - 0.526	57 - 71

Concerning the sedimentation studies, a decrease of about 50% of the smallest sizes was observed after 1 hour and a pronounced intensity increase of bigger sizes after 24h. These results confirm the strong influence of sedimentation in agglomerates formation. The subsequent analysis by FEG-SEM suggests that the agglomerates probably do not correspond to nanoparticles. From the images obtained, the most similar with spherical structures that may correspond to nanoparticles is represented in Figure 4.11, with diameters around 100 nm. However, given the surrounding agglomeration, it is not possible to make reliable conclusions regarding the nature of those structures.

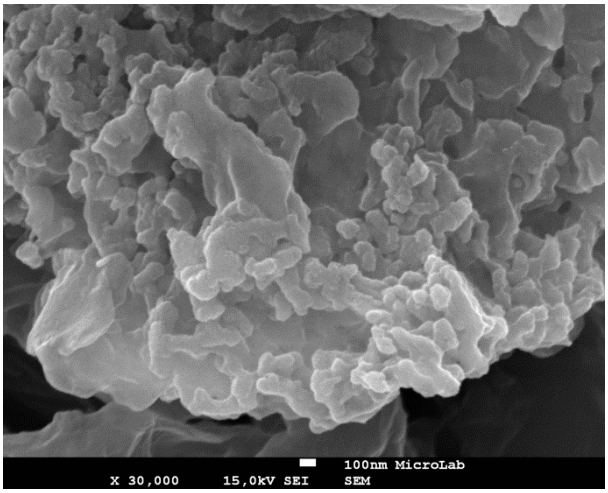

Figure 4.11 – FEG-SEM image of structures that may correspond to nanoparticles obtained by nanoprecipitation of mPEG-co-PCL and PEITC (Scale bar: 100nm).

The remaining images obtained by FEG-SEM show larger structures, with no defined shape. Some examples are represented in Figure 4.12.

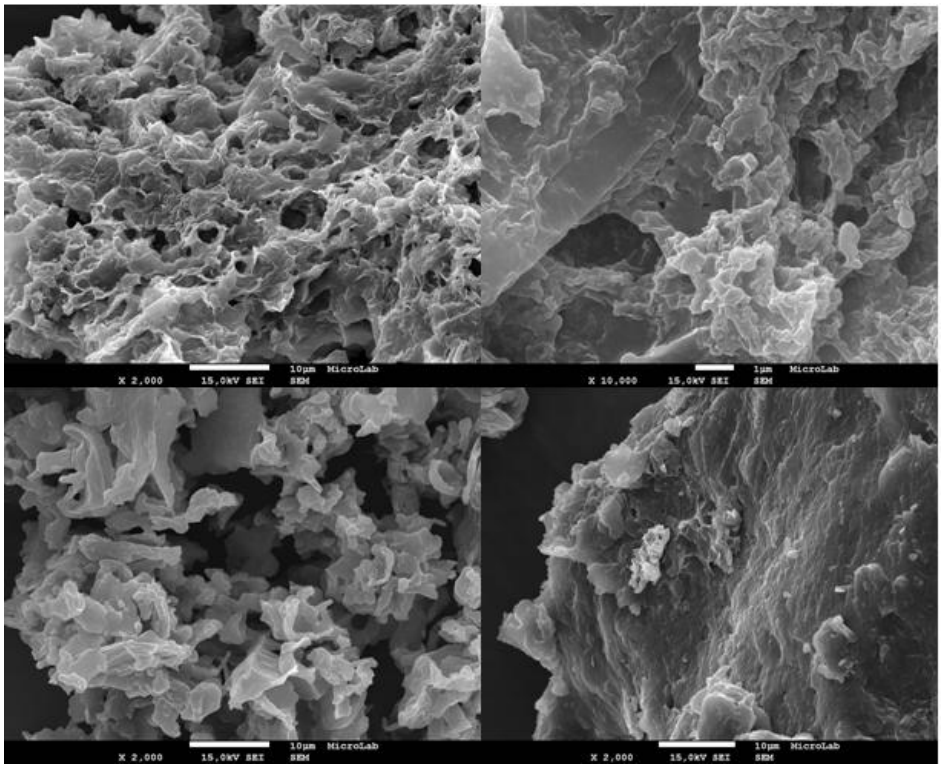

Figure 4.12 - FEG-SEM image of non-defined structures, obtained by nanoprecipitation of mPEG-co-PCL and PEITC (Scale bar: left top - 10 µm; left bottom - 10 µm; right top - 1 µm; right bottom – 10 µm).

As observed, there is no uniformity between the structures. Images from different aliquots of the same sample show an undefined arrangement. In most cases it appears as films or networks, which may correspond to impurities or contaminants. Alternatively, it can result from unexpected interactions involving the reactants used in the procedure (drug, copolymer and solvents) which may have interfered with the nanoprecipitation procedure. It is not possible to conclude whether there was an efficient encapsulation by nanoprecipitation since the larger structures can be 'masking' the existence of nanoparticles. To clarify these hypotheses, further developments and optimizations need to be designed and performed. However, given the available time and since the concurrent development of nanoparticles of chitosan-collagenase showed promising results, the supplementary developments concerning the encapsulation of PEITC in mPEG-co-PCL was scheduled for future tasks.

4.3. Chitosan and chitosan-collagenase crosslinked nanoparticles

The synthesis of chitosan nanoparticles was reproduced as control, to compare the results obtained in the first developments concerning size and morphology and to verify the influence of collagenase incorporation in the loading and release assays patterns of chitosan nanoparticulate systems. After reproduction of chitosan NPs and comparative evaluation needed to consider the chitosan-collagenase

nanosystems as reproducible and promising, the experimental developments were directed to the individual optimization of the chitosan-collagenase nanoparticles.

The synthesis of chitosan and chitosan-collagenase nanoparticles was submitted to several stages of optimization, mainly in terms of scale-up, to obtain significant amounts.

The final yield of the each synthesis was calculated by the formula:

$$\%\ \text{yield} = \frac{\text{Nanoparticles dry weight}}{\text{Reactants weight}} \cdot 100$$

The reactants used in the synthesis were chitosan and genipin in the case of chitosan nanoparticles and chitosan, collagenase and genipin in the case of chitosan-collagenase nanoparticles.

In the first syntheses, collectable amounts of nanoparticles were not obtained, so it was not possible to calculate the final yield for those stages. The first measurable amounts obtained by initial scale-up, had yields around 10% for chitosan NPs and 9% for chitosan-collagenase NPs. Further optimization regarding the system of interest – chitosan-collagenase NPs – gave yields from 58 to 65%.

Since chitosan-collagenase nanoparticles are a novel system, never synthesized before, the first step after synthesis was to confirm to reproducibility of the procedure for this new system, by comparison to the standard – chitosan NPs. The analysis by DLS it is not adequate for these samples, because the nanoparticles are intrinsically coloured. The characterization regarding size and morphology was obtained by FEG-SEM. The first output, for samples dried by lyophilisation is represented in Figure 4.13.

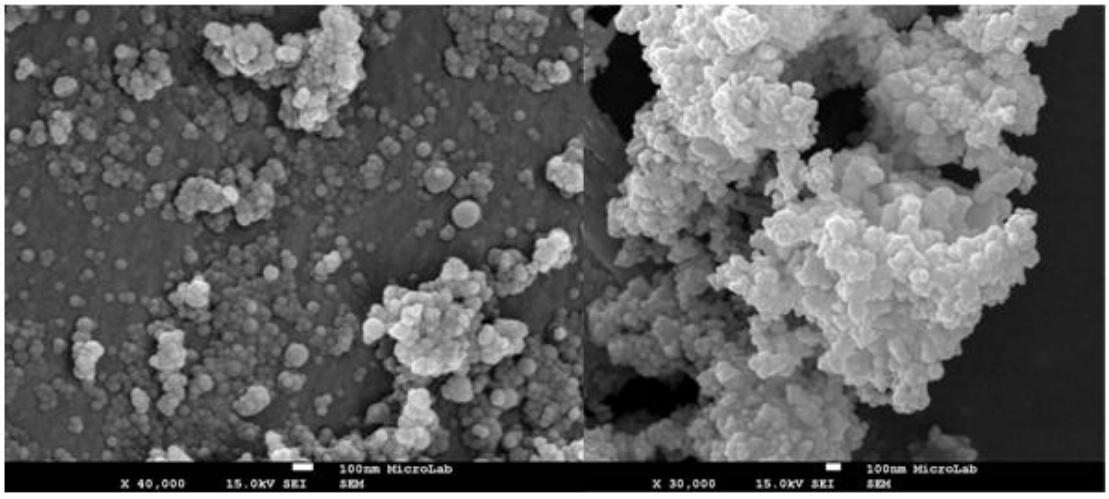

Figure 4.13 – FEG-SEM images of nanoparticles dried by lyophilisation. Left – chitosan nanoparticles; right – chitosan-collagenase nanoparticles (Scale bar: 100nm).

As observed in the images, it was possible to accurately reproduce spherical chitosan nanoparticles with monodisperse sizes, in a range mostly below 50 nm (Figure 4.13, left), as described by the authors followed for this synthesis (Arteche Pujana et al., 2013). Concerning the chitosan-collagenase NPs (Figure 4.13, right), the structures are not clearly defined, thereby, it is difficult to obtain an unambiguous characterisation.

During synthesis optimization stages, regarding increased yield and time saving, other methodologies were tested for nanoparticles isolation and drying. Rotavapor equipment was used for vacuum-accelerated solvent evaporation and further surfactant elimination by washing with diethylether. This approach was designed to reduce the manipulation steps needed to wash and dry the nanoparticles, since it avoids the initial washing cycles needed for lyophilisation and significantly reduces the drying time (72 hours by lyophilisation and less than 24 hours using rotavap). The images obtained for the samples dried using this technique, are represented in Figure 4.14.

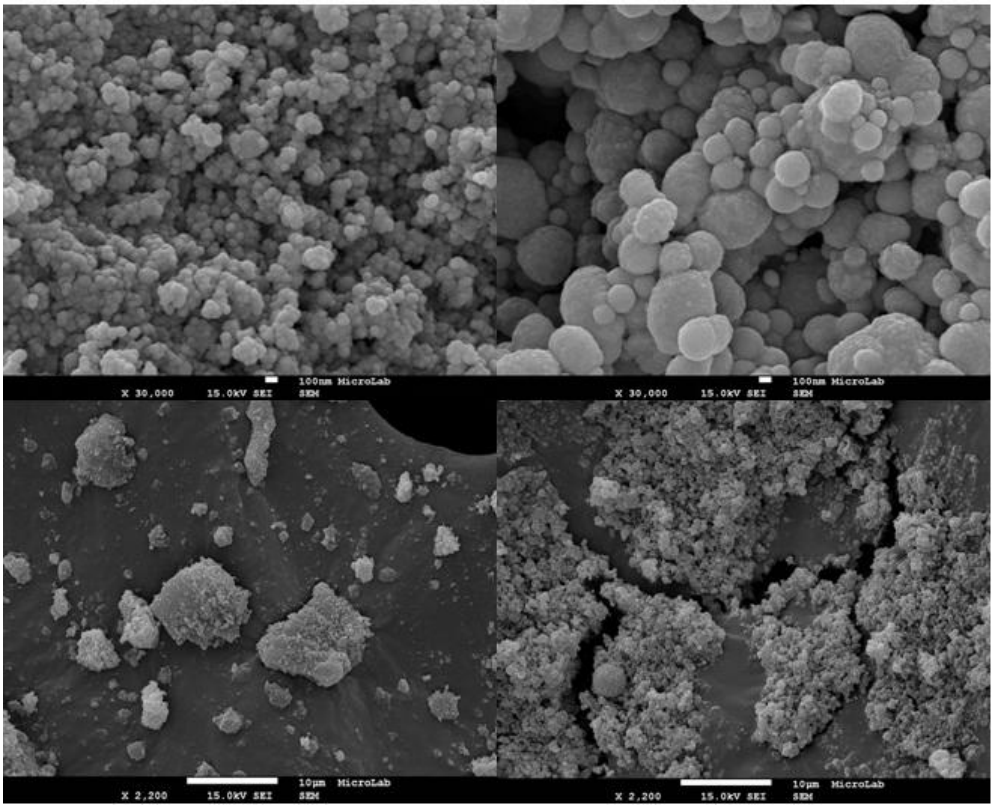

Figure 4.14 - FEG-SEM images of nanoparticles dried using rotary evaporation. Left – chitosan nanoparticles; right – chitosan-collagenase nanoparticles (Scale bar: top - 100 nm; bottom - 10 µm).

The chitosan NPs (Figure 4.14, left) remained similar to those previously obtained, in terms of size and morphology, but presented a highly agglomerated organization. In turn, the chitosan-collagenase nanoparticles obtained in this synthesis (Figure 4.14, right) presented a well defined

spherical structure, with higher and more dispersed sizes, in the range of 100 to 500 nm. Observing the image with higher magnification (right, top, 100 nm scale), it is clear the rough surface of chitosan-collagenase NPs, which may indicate fusion phenomena. Besides, these NPs also present a high agglomeration degree, which suggests the presence of surfactant, highly viscous, acting as a resin. The drying by solvent evaporation concentrates all the surfactant, which highly difficults its removal, this being the major drawback of rotavap drying. Additionally, although nanoparticles may be stable at the temperature applied in this technique (37°C), calorimetric studies should be done to confirm their thermal stability.

An alternative approach, aiming for nanoparticles isolation and drying in a one-step procedure, was nanoparticles vacuum filtration using an adsorbent membrane - NADIR UP-10. This membrane presented stable parameters in terms of colour, size, thickness, weight and malleability for adsorption of the solvents used in inverse microemulsion. The membrane is impermeable to the nanoparticles, isolating them from the microemulsion by adsorption of the liquid phase, which is pulled out by the vacuum system. Micrographs of chitosan and chitosan-collagenase nanoparticulate samples dried by this method are shown in Figure 4.15.

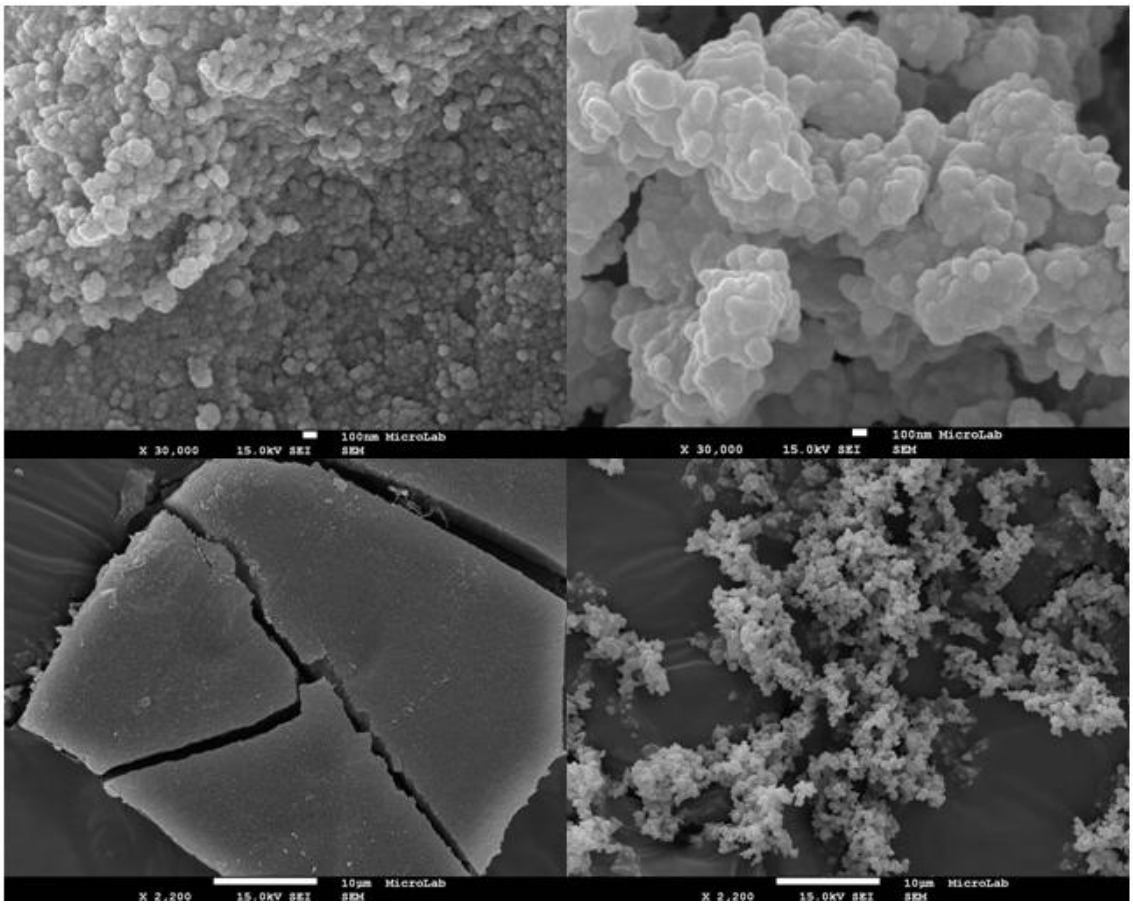

Figure 4.15 - FEG-SEM images of nanoparticles dried using NADIR UP-10 membrane. Left – chitosan nanoparticles; right – chitosan-collagenase nanoparticles (Scale bar: top – 100 nm; bottom - 10 µm).

Chitosan nanoparticles showed similar characteristics (Figure 4.15, left), compared to previous syntheses. Concerning chitosan-collagenase, there were technical problems during the synthesis that compromised the efficient formation and isolation of nanoparticles. The images (Figure 4.15, right) show agglomerated structures tending to spherical shape, suggesting an incomplete synthesis.

Despite the prospects of NADIR-UP 10 membrane, its application in the dry procedure was not continued due to the unexpected drawbacks detected. Even with the combined action of membrane adsorption and vacuum, a high percentage of surfactant was detected, involving the nanoparticles in a matrix-like structure, as is possible to observe in the lower magnification image of chitosan (Figure 4.15, left, bottom, 10 µm scale). Moreover, the membrane is very expensive, with restricted utilization and has low processing capacity for the purpose (slow process for small sample amounts).

The last tested procedure regarding the obtention of solvent/surfactant-free nanoparticles was simply based on washing cycles with ethanol and diethylther. The synthesized nanoparticles dried by this process are represented in Figure 4.16.

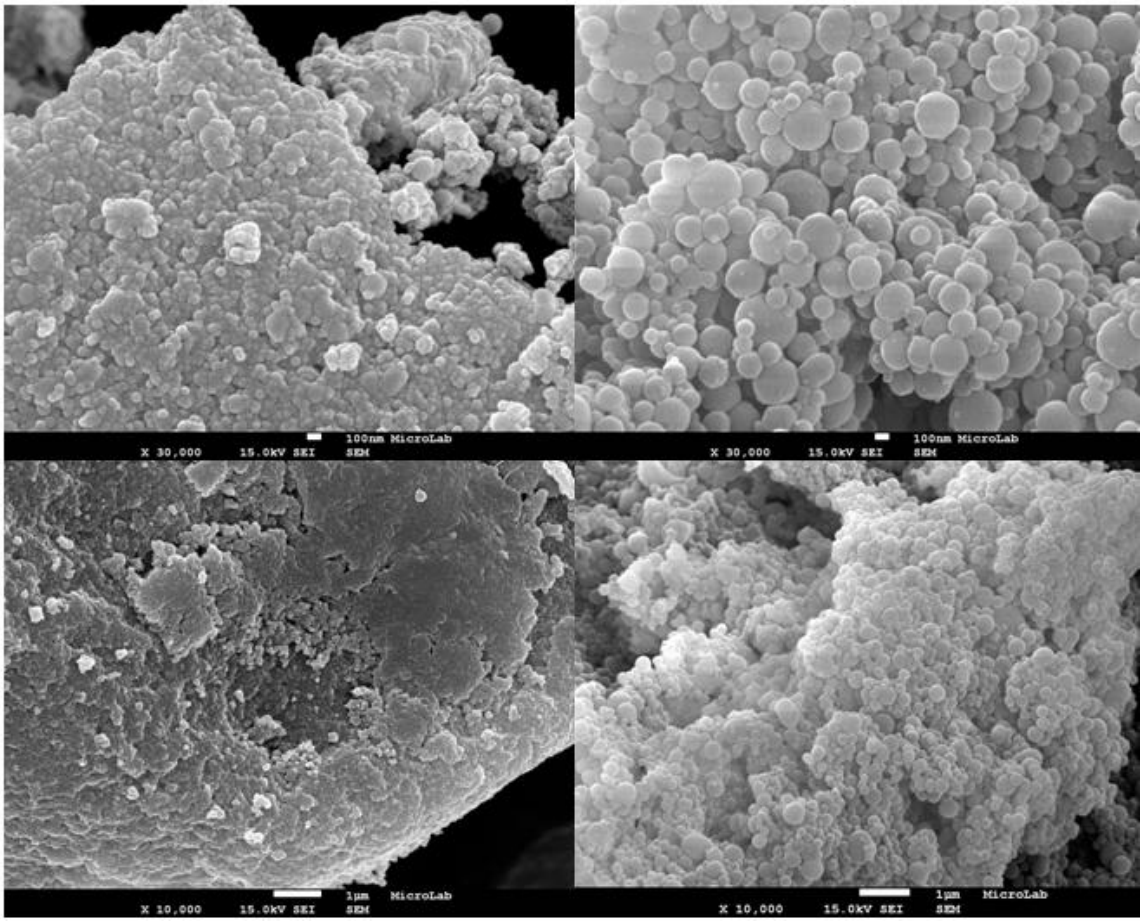

Figure 4.16 - FEG-SEM images of nanoparticles washed and dried using ethanol and diethylether. Left – chitosan nanoparticles; right – chitosan-collagenase nanoparticles (Scale bar: top - 100 nm; bottom - 1 µm).

The chitosan NPs features remained identical, although highly agglomerated, probably due to inefficient surfactant elimination. However, for chitosan-collagenase nanoparticles, this procedure was the most favourable, showing a lower agglomeration degree. In terms of size and morphology, this batch of chitosan-collagenase nanoparticles presents spherical shape and size ranges around 100 to 500 nm.

Summarizing the characterization by FEG-SEM, the nanoparticles synthesized presented spherical forms, with monodisperse sizes for chitosan NPs, under 50 nm, and broad size ranges for chitosan-collagenase NPs, ranging from 100 to 500 nm.

The obtention of visible alterations in nanoparticles characteristics by collagenase addition, suggest an efficient incorporation of collagenase in the nanoparticulate system. Comparing to chitosan NPs standards, the chitosan-collagenase nanoparticles presented larger sizes, different colour and less adhesion (easier dispersion).

4.3.1. Load and release of 5-fluorouracil

The encapsulation of 5-fluorouracil (5-Fu) in these nanoparticles was chosen since it is a chemotherapeutic agent, widely used in the treatment of colorectal cancer, which is the target of the work in development.

The encapsulation efficiency (EE) was calculated by the formula:

$$EE\ (\%) = \frac{[5\text{-Fu}]_{total} - [5\text{-Fu}]_{supernatant}}{[5\text{-Fu}]_{total}} \cdot 100$$

The $[5\text{-Fu}]_{total}$ refers to the concentration of 5-Fu added to the nanoparticles and the $[5\text{-Fu}]_{supermatant}$ indicates the concentration of 5-Fu in the supernatant after nanoparticles centrifugation. The EE obtained in the first load assays and the remaining important parameters are summarized in Table 4.5.

Table 4.5 – Estimated parameters after 5-fluorouracil encapsulation in chitosan and chitosan-collagenase nanoparticles, at a pH of 5.5.

	EE (%)	[5-Fu] (µM)	µg 5-Fu/mg NPs
Chitosan	]38;42[	]58;64[	[7.6 ; 8.3]
Chitosan-collagenase	[34;37[	]51;56[	[6.7 ; 7.2]

Note: These data refers to a standard nanoparticles concentration of 1 mg/mL.

The 5-Fu loading data obtained for both nanosystems is similar, with slightly higher values for chitosan NPs. Since the loads are made by swelling of the nanoparticles network due to chitosan pH

sensitivity, it is normal to obtain higher encapsulation efficiency in chitosan nanoparticles in comparison to chitosan-collagenase, that have lower chitosan amounts.

The subsequent release assays suggests null drug liberation at pH 5.5, which may indicate an insufficient swelling of the network. However, in the cellular context, there are other conditions that can promote the release (enzymes, temperature, etc.). The values of average inhibiting concentration (IC50) given by the IPOLFG (Instituto Português de Oncologia de Lisboa Francisco Gentil) partners for the HT29 cell line (human colorectal adenocarcinoma cell line) were 2.39 μM for proliferation and 11.79 μM for viability. Since the 5-Fu loaded concentration is higher than IC50 values, loaded nanoparticles were prepared and tested *in vitro* in that cell line, by the Colon Pathology Study Group (IPOLFG). The preliminary assays were not conclusive due to high agglomeration of nanoparticles and interference of its intrinsic colour in the standard procedures. Presently, optimization is being done to bypass those problems.

In parallel, studies regarding the network swelling were developed, only for the novel system, chitosan-collagenase nanoparticles, since its reproducibility was confirmed by comparative analysis with the chitosan NPs, used as control.

In the previous syntheses, excess amounts of genipin (genipin:polymer ratio of 10:1) were used to guarantee a maximum crosslinking. To evaluate the network swelling constraint by influence of the crosslinking degree, new syntheses were reproduced using 10%, 20% and 40% of genipin amounts, corresponding to 1:10; 1:5 and 2:5 ratios of genipin:polymer, respectively. To simultaneously evaluate the influence of acidity in the network swelling, the nanoparticles load and release were tested at the standard pH 5.5 and at pH 3. These studies were done in fixed time periods. The data regarding encapsulation efficiency, drug loaded concentration and relative amount of 5-Fu and nanoparticles, are summarized in Table 4.6.

Table 4.6 - Estimated parameters obtained by 5-fluorouracil encapsulation at pH 5.5 and 3, in chitosan-collagenase nanoparticles, synthesized using genipin:polymer ratios of 1:10, 1:5 and 2:5.

Genipin:polymer ratio	pH	EE (%)	$[5\text{-Fu}]_{loaded}$ (μM)	μg 5-Fu/mg NPs
1:10	3	73	214.37	8.42
	5.5	60	137.57	6.03
1:5	3	62	182.00	7.35
	5.5	64	147.01	5.40
2:5	3	65	191.44	9.22
	5.5	65	149.71	6.81

Note: These data refers to a nanoparticles concentration around 3 mg/mL.

The parameter used for comparative analysis was the μg 5-Fu per mg of nanoparticles (μg 5-Fu/mg NPs) because the EE does not consider the nanoparticles concentration used in the loading procedure, being inadequate for an equivalent comparison. The values were similar to those previously obtained for chitosan and chitosan-collagenase NPs, ranging from 5 to 9 μg 5-Fu per mg of NPs.

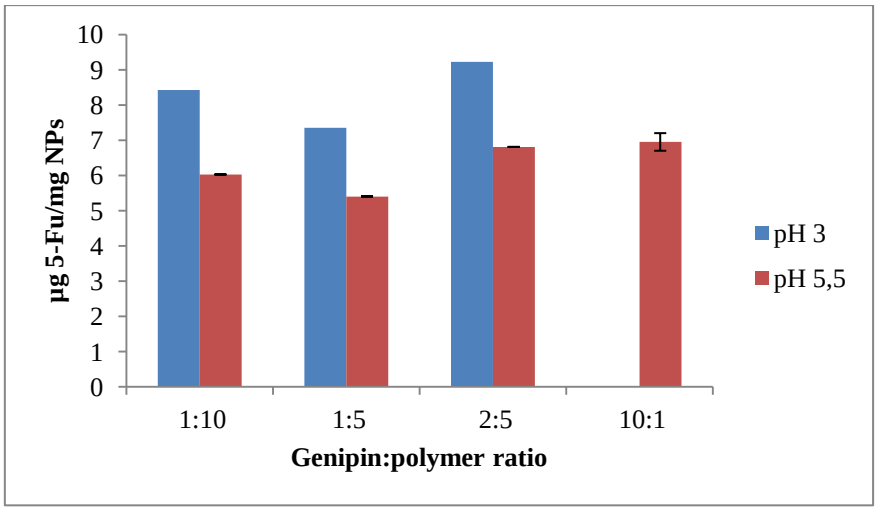

Figure 4.17 – Graphical representation of 5-Fu loading outcomes for chitosan-collagenase nanoparticles synthesized with a genipin:polymer ratio of 1:10, 1:5, 2:5 and 10:1.

The encapsulation results show higher loads for pH 3 than pH 5.5, suggesting that the network swelling is enhanced by acidity increase.

Besides, higher encapsulation values were obtained for chitosan-collagenase NPs with higher crosslinker content, although there is no linear trend with crosslinker increase.

The release efficiency (RE) was calculated by the formula:

$$RE\ (\%) = \frac{[\text{5-Fu}]_{\text{supernatant}}}{[\text{5-Fu}]_{\text{loaded}}} \cdot 100$$

The release data collected regarding the tested pH and crosslinking conditions are summarized in Table 4.7.

Table 4.7 - Estimated parameters obtained by 5-fluorouracil release at pH 5.5 and 3, from the previously loaded chitosan-collagenase nanoparticles, synthesized using genipin:polymer ratios of 1:10, 1:5 and 2:5.

Genipin:polymer ratio	Load pH	Release pH	RE (%)	[5-Fu] (µM)	µg 5-Fu/mg NPs
1 : 10	3	3	10.1	21.76	0.86
		5.5	1.9	4,00	0.16
	5.5	3	11.6	16,00	0.70
		5.5	5.9	8.07	0.35
1 : 5	3	3	4.4	8,00	0.32
		5.5	6.6	12.07	0.49
	5.5	3	15.6	22.91	0.84
		5.5	4.5	6.69	0.25
2 :5	3	3	4.8	9.15	0.44
		5.5	2.8	5.38	0.26
	5.5	3	5.3	8,00	0.37
		5.5	0.9	1.31	0.06

As shown in Table 2.1, the released amounts of 5-fluoroutacil per mg of NPs were low. However, those values can be analysed for comparative purposes regarding the study of pH and crosslinking influence in nanoparticles swelling. The results are graphically represented in Figure 4.18.

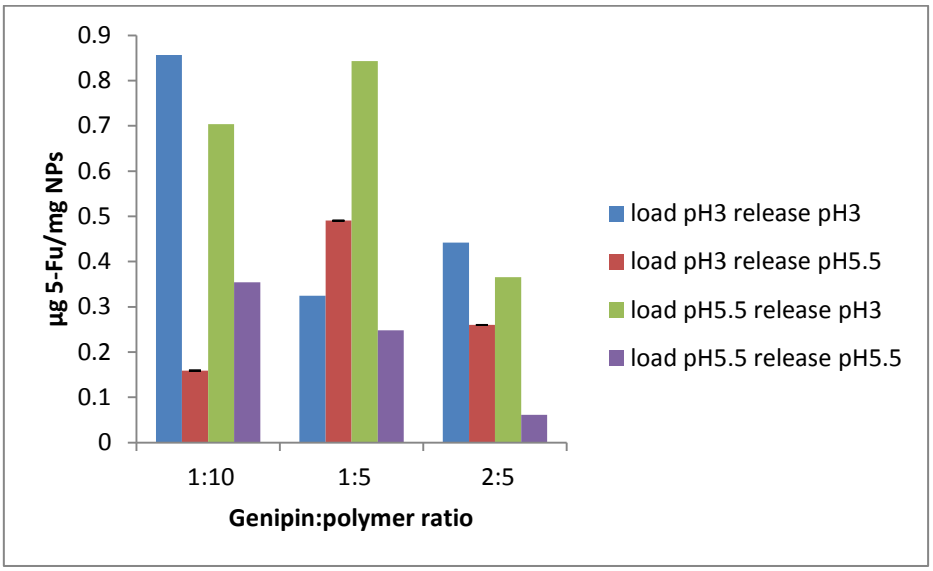

Figure 4.18 - Graphical representation of 5-Fu release outcomes from previously loaded chitosan-collagenase nanoparticles synthesized with a genipin:polymer ratio of 1:10, 1:5, 2:5 and 10:1.

Concerning the crosslinking influence, the system with high crosslinker content (genipin:polymer ratio of 2:5) presented, in general, the higher loads (Figure 4.17) and the lower release values (Figure 4.18). This suggests that the drug entrapment is influenced not only by the network swelling, but also by its internal organisation. Nanoparticles with lower crosslinking degrees form networks with higher porosity, making drug migration easier. Larger pores confer less entrapment capacity to the network but higher release efficiency. Since that behaviour is not uniform for linear crosslinker variations, further developments to achieve the most favourable genipin:polymer ratio in terms of drug entrapment and release rates should be done. For medical purposes, it is crucial to find the best equilibrium between the drug dose and its sustained and controlled release.

Regarding pH, it was observed that, in most cases, the load and release at pH 3 promoted higher drug liberation and load and release at pH 5.5 presented the lower liberation values. The data in Figure 4.18, were rearranged to allow a detailed analysis regarding pH influence - Figure 4.19.

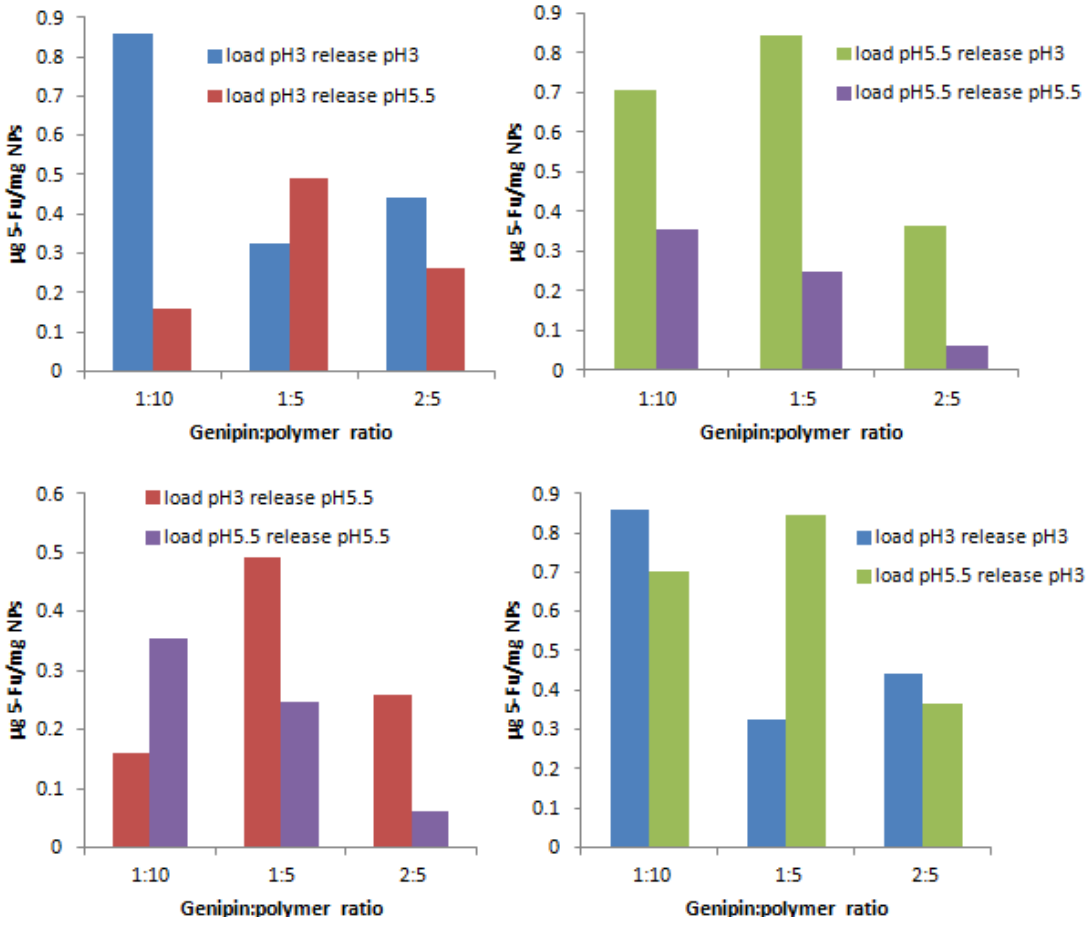

Figure 4.19 - Graphical representation of 5-Fu release outcomes from chitosan-collagenase nanoparticles submitted to equal load pH (top) and equal release pH (bottom).

Analysing independently the release outcomes for equal load pH and equal release pH, a major release enhancement for nanoparticles in which the load and/or release occurred at pH 3 is observed.

In summary, according to the observations regarding pH, it is possible to postulate that network swelling increases with acidity. The crosslinking degree influences the network swelling, but it is not yet possible to define a pattern.

5. CONCLUSIONS

The presented work focused on the concurrent development of two polymeric nanoparticulate systems, mPEG-co-PCL and chitosan-collagenase nanoparticles, aiming to target metastatic colorectal cancer. The encapsulation of PEITC in mPEG-co-PCL NPs was tested for the first time, applying a green approach, using empty and C6-loaded mPEG-co-PCL NPs as control. In parallel, a chemical approach was applied for the development of chitosan-collagenase nanoparticles, as a novel system, using chitosan NPs as control. Encapsulation and release assays were performed for this system, using 5-fluorouracil.

Regarding the mPEG-co-PCL nanoparticles, it was possible to reproduce the empty nanoparticles with parameters in agreement with the literature. The C6-loaded nanoparticles presented a size range higher than the procedure-based publications and high contents of non-encapsulated coumarin-6, suggesting low encapsulation efficiency. In turn, the results obtained for PEITC encapsulation in mPEG-co-PCL does not allow to reliably confirm an efficient synthesis of PEITC-loaded nanoparticles, needing further optimization. Since the development of this system did not present reproducibility in the predicted time, and given the promising results obtained in parallel for chitosan-collagenase nanoparticles, the remaining tasks focused on this novel system.

The chitosan-collagenase nanoparticles were efficiently developed, revealing spherical shape and broad sizes, ranging from 100 to 500 nm, in comparison to chitosan-control nanoparticles, reproduced in sizes under 50 nm. It was possible to optimize the syntheses yield up to values around 65%.

Concerning the encapsulation and release assays, it was possible to obtain loads ranging from 5 to 9 µg of 5-Fu per mg of nanoparticles, acceptable to submit to *in vitro* assays, already initiated. However the release was significantly low, in ranges of 0.06 to 0.86 5-Fu µg per NPs mg. The study of the influence of pH and crosslinking degree in nanoparticles network swelling suggests swelling enhancement in more acidic pH and lower crosslinking percentage. In turn, the results obtained for different crosslink contents support the hypothesis of an opposite effect for loading and release, in which crosslinking enhancement confers to the network higher entrapment capacity but lower release efficiency.

The development of both PEITC-loaded mPEG-co-PCL and chitosan-collagenase nanosystems is expected to continue in future work, as further described in the next section.

6. FUTURE WORK

The future tasks include two different work plans, comprising PEITC-loaded mPEG-co-PCL and chitosan-collagenase nanoparticles, respectively.

The development of PEITC-loaded mPEG-co-PCL nanoparticles is in preliminary stages, needing full optimization from the initial synthesis steps to the characterization.

Concerning chitosan-collagenase nanoparticles, that has been the main target of the work developed during this thesis, it is necessary to further characterize the nanoparticulate system. A complete physicochemical characterization will allow to direct its features to the target goals in a more profitable perspective.

Moreover, the load and release capacity of the nanosystems needs to be further studied in several parameters. Additional tests regarding pH and crosslinking influence have to be done to validate the postulated hypotheses. Assays for studying this field had already been designed, including time variable, to achieve an equilibrium between nanoparticles drug content and its release efficiency, with the potential to promote a sustained and controlled release in a pharmacological perspective.

Since chitosan-collagenase nanoparticles are already involved in *in vitro* assays, and preliminary results reveal agglomeration as an obstacle, current developments are focused on the study of chitosan-collagenase nanoparticles stability in solution.

Besides, it is planned for a near future the encapsulation of curcumin, a natural compound with antitumor features, proven potential for chemotherapeutic treatment of colorectal cancer (Chauhan, 2002) and synergetic effect when combined with 5-fluorouracil (Toden et al., 2014). The projected tasks aim to test *in vitro* the individual effects of 5-fluorouracil and curcumin, their synergy and the contribution of their individual and combined encapsulation in chitosan-collagenase nanoparticles, in terms of targeting and release efficiency.

Furthermore, since both mPEG-co-PCL and chitosan-collagenase nanoparticles were planned to be specialized for specific recognition of metastasis from colorectal cancer, functionalization pathways are being prepared for surface modification with a peptide to recognize a biomarker overexpressed in primary and metastatic colorectal carcinoma cells.

A manuscript is being prepared for chitosan-collagenase nanoparticles, expected to be submitted early next year.

7. REFERENCES

Articles

Anitha, A., Deepa, N., Chennazhi, K. P., Lakshmanan, V. K., & Jayakumar, R. (2014). Combinatorial anticancer effects of curcumin and 5-fluorouracil loaded thiolated chitosan nanoparticles towards colon cancer treatment. *Biochimica et Biophysica Acta - General Subjects*, *1840*(9), 2730–2743. http://doi.org/10.1016/j.bbagen.2014.06.004

Arteche Pujana, M., Perez-Alvarez, L., Cesteros Iturbe, L. C., & Katime, I. (2014). PH-sensitive chitosan-folate nanogels crosslinked with biocompatible dicarboxylic acids. *European Polymer Journal*, *61*, 215–225. http://doi.org/10.1016/j.eurpolymj.2014.10.007

Arteche Pujana, M., Pérez-Álvarez, L., Cesteros Iturbe, L. C., & Katime, I. (2013). Biodegradable chitosan nanogels crosslinked with genipin. *Carbohydrate Polymers*, *94*(2), 836–842. http://doi.org/10.1016/j.carbpol.2013.01.082

Aruna, U., Rajalakshmi, R., Indira Muzib, Y., Vinesha, V., Sushma, M., Vandana, K., Vijay Kumar, N., Rangampet, A. (2013). Role of Chitosan Nanoparticles in Cancer Therapy. *International Journal of Innovative Pharmaceutical Research*, *4*(3), 318–324.

Baetke, S. C., Lammers, T., & Kiessling, F. (2015). Applications of nanoparticles for diagnosis and therapy of cancer. *British Journal of Radiology*, *88*(1054). http://doi.org/10.1259/bjr.20150207

Baimark, Y. (2009). Surfactant-Free Nanospheres of Methoxy Poly (Ethylene Glycol)-b-Poly (ε-Caprolactone) for Controlled Release of Ibuprofen. *Journal of Applied Sciences*, *9*(12), 2287–2293. http://doi.org/10.1017/CBO9781107415324.004

Baimark, Y., & Srisuwan, Y. (2012). Biodegradable nanoparticles of methoxy poly(ethylene glycol)-b-poly(d, l-lactide)/methoxy poly(ethylene glycol)- b-poly(ϵ-caprolactone) blends for drug delivery. *Nanoscale Research Letters*, *7*(1), 271. http://doi.org/10.1186/1556-276X-7-271

Cerchiara, T., Abruzzo, A., Di Cagno, M., Bigucci, F., Bauer-Brandl, A., Parolin, C., Vitali, B., Gallucci, M. C., Luppi, B. (2015). Chitosan based micro- and nanoparticles for colon-targeted delivery of vancomycin prepared by alternative processing methods. *European Journal of Pharmaceutics and Biopharmaceutics*, *92*, 112–119. http://doi.org/10.1016/j.ejpb.2015.03.004

Chauhan, D. P. (2002). Chemotherapeutic potential of curcumin for colorectal cancer. *Current Pharmaceutical Design*, *8*(19), 1695–706. http://doi.org/10.2174/1381612023394016

Choi, H. S., Liu, W., Misra, P., Tanaka, E., Zimmer, J. P., Itty Ipe, B., Bawendi, M. G., Frangioni, J. V. (2007). Renal clearance of nanoparticles. *Nat. Biotechnol.*, *25*(10), 1165–1170. http://doi.org/10.1038/nbt1340

Danafar, H., & Schumacher, U. (2016). MPEG–PCL copolymeric nanoparticles in drug delivery systems. *Cogent Medicine*, *3*(1), 1142411. http://doi.org/10.1080/2331205X.2016.1142411.

Deng, X., Cao, M., Zhang, J., Hu, K., Yin, Z., Zhou, Z., Xiao, X., Yang, Y., Sheng, W., Wu, Y., Zeng, Y. (2014). Hyaluronic acid-chitosan nanoparticles for co-delivery of MiR-34a and doxorubicin in therapy against triple negative breast cancer. *Biomaterials*, *35*(14), 4333–4344. http://doi.org/10.1016/j.biomaterials.2014.02.006

Feng, C., Li, J., Kong, M., Liu, Y., Cheng, X. J., Li, Y., Park, H. J., Chen, X. G. (2015). Surface charge effect on mucoadhesion of chitosan based nanogels for local anti-colorectal cancer drug delivery. *Colloids and Surfaces B: Biointerfaces*, *128*, 439–447. http://doi.org/10.1016/j.colsurfb.2015.02.042

Ferlay, J., Steliarova-Foucher, E., Lortet-Tieulent, J., Rosso, S., Coebergh, J. W. W., Comber, H., Forman, D., Bray, F. (2013). Cancer incidence and mortality patterns in Europe: Estimates for 40 countries in 2012. *European Journal of Cancer*, *49*(6), 1374–1403. http://doi.org/10.1016/j.ejca.2012.12.027

Goodman, T. T., Olive, P. L., & Pun, S. H. (2007). Increased nanoparticle penetration in collagenase-treated multicellular spheroids. *International Journal of Nanomedicine*, *2*(2), 265–274.

Guan, M., Zhou, Y., Zhu, Q. L., Liu, Y., Bei, Y. Y., Zhang, X. N., & Zhang, Q. (2012). N-trimethyl chitosan nanoparticle-encapsulated lactosyl-norcantharidin for liver cancer therapy with high targeting efficacy. *Nanomedicine: Nanotechnology, Biology, and Medicine*, *8*(7), 1172–1181. http://doi.org/10.1016/j.nano.2012.01.009

Haegele, J., Duschka, R., Graeser, M., Luedtke-Buzug, K., Schaecke, C., Panagiotopoulos, N., Buzug, T. M., Barkhausen, J., Vogt, F. M. (2014). Magnetic particle imaging: Kinetics of the intravascular signal in vivo. *2013 International Workshop on Magnetic Particle Imaging, IWMPI 2013*, 4203–4209. http://doi.org/10.1109/IWMPI.2013.6528350

Hafner, A., Lovrić, J., Lakoš, G. P., & Pepić, I. (2014). Nanotherapeutics in the EU: an overview on current state and future directions. *International Journal of Nanomedicine*, *9*, 1005–23. http://doi.org/10.2147/IJN.S55359

Hamman, J. H. (2010). Chitosan based polyelectrolyte complexes as potential carrier materials in drug delivery systems. *Marine Drugs*. http://doi.org/10.3390/md8041305

Hang, Z., Cooper, M. A., & Ziora, Z. M. (2016). Platinum-based anticancer drugs encapsulated liposome and polymeric micelle formulation in clinical trials. *Biochemical Compounds*, *4*(1), 1. http://doi.org/10.7243/2052-9341-4-2

Je, J. Y., & Kim, S. K. (2012). Chitosan as Potential Marine Nutraceutical. *Advances in Food and Nutrition Research*, *65*, 121–135. http://doi.org/10.1016/B978-0-12-416003-3.00007-X

Jin, S. E., Jin, H. E., & Hong, S. S. (2014). Targeted delivery system of nanobiomaterials in anticancer therapy: From cells to clinics. *BioMed Research International*, *2014*. http://doi.org/10.1155/2014/814208

Kato, M., Hattori, Y., Kubo, M., & Maitani, Y. (2012). Collagenase-1 injection improved tumor distribution and gene expression of cationic lipoplex. *International Journal of Pharmaceutics*, *423*(2), 428–434. http://doi.org/10.1016/j.ijpharm.2011.12.015

Khatik, R., Mishra, R., Verma, A., Dwivedi, P., Kumar, V., Gupta, V., Paliwal, S. K., Mishra, P. R., Dwivedi, A. K. (2013). Colon-specific delivery of curcumin by exploiting Eudragit-decorated chitosan nanoparticles in vitro and in vivo. *Journal of Nanoparticle Research*, *15*(9). http://doi.org/10.1007/s11051-013-1893-x

Lee, S. J., Min, H. S., Ku, S. H., Son, S., Kwon, I. C., Kim, S. H., & Kim, K. (2014). Tumor-targeting glycol chitosan nanoparticles as a platform delivery carrier in cancer diagnosis and therapy. *Nanomedicine (Lond)*, *9*(11), 1697–1713. http://doi.org/10.2217/nnm.14.99

Lins, L. C., Bazzo, G. C., Barreto, P. L. M., & Pires, A. T. N. (2014). Composite PHB/Chitosan microparticles obtained by spray drying: Effect of chitosan concentration and crosslinking agents on drug relesase. *Journal of the Brazilian Chemical Society*, *25*(8), 1462–1471. http://doi.org/10.5935/0103-5053.20140129

Long, W., Gill, C. S., Choi, S., & Jones, C. W. (2010). Recoverable and recyclable magnetic nanoparticle supported aluminium isopropoxide for ring-opening polymerization of epsilon-caprolactone. *Dalton Transactions (Cambridge, England : 2003)*, *39*(6), 1470–2. http://doi.org/10.1039/b923622h

Malhotra, M., Tomaro-Duchesneau, C., Saha, S., & Prakash, S. (2013). Systemic siRNA delivery via peptide-tagged polymeric nanoparticles, targeting PLK1 gene in a mouse xenograft model of colorectal cancer. *International Journal of Biomaterials*, *2013*. http://doi.org/10.1155/2013/252531

Malik, M. A., Wani, M. Y., & Hashim, M. A. (2012). Microemulsion method: A novel route to synthesize organic and inorganic nanomaterials. 1st Nano Update. *Arabian Journal of Chemistry*, *5*(4), 397–417. http://doi.org/10.1016/j.arabjc.2010.09.027

Marin, E., Briceño, M. I., & Caballero-George, C. (2013). Critical evaluation of biodegradable polymers used in nanodrugs. *International Journal of Nanomedicine*, *8*, 3071–3091. http://doi.org/10.2147/IJN.S47186

Masi, G., Fornaro, L., Caparello, C., & Falcone, A. (2011). Liver metastases from colorectal cancer: how to best complement medical treatment with surgical approaches. *Future Oncology (London, England)*, *7*(11), 1299–1323. http://doi.org/10.2217/fon.11.108

Maya, S., Sarmento, B., Lakshmanan, V. K., Menon, D., Seabra, V., & Jayakumar, R. (2014). Chitosan cross-linked docetaxel loaded EGF receptor targeted nanoparticles for lung cancer cells. *International Journal of Biological Macromolecules*, *69*, 532–541. http://doi.org/10.1016/j.ijbiomac.2014.06.009

Mehrotra, A., Nagarwal, R. C., & Pandit, J. K. (2011). Lomustine loaded chitosan nanoparticles: characterization and in-vitro cytotoxicity on human lung cancer cell line L132. *Chemical & Pharmaceutical Bulletin*, *59*(3), 315–320. http://doi.org/10.1248/cpb.59.315

Minost, A., Delaveau, J., Bolzinger, M. A., Fessi, H., & Elaissari, A. (2012). Nanoparticles via nanoprecipitation process. *Recent Patents on Drug Delivery and Formulation*, *6*(3), 250–258. http://doi.org/10.2174/187221112802652615

Moilanen, J. M., Kokkonen, N., Löffek, S., Väyrynen, J. P., Syväniemi, E., Hurskainen, T., Mäkinen, M., Klintrup, K., Mäkelä, J., Sormunen, R., Bruckner-Tuderman, L., Autio-Harmainen, H., Tasanen, K. (2015). Collagen XVII expression correlates with the invasion and metastasis of colorectal cancer. *Human Pathology*, *46*(3), 434–442. http://doi.org/10.1016/j.humpath.2014.11.020

Murty, S., Gilliland, T., Qiao, P., Tabtieng, T., Higbee, E., Al Zaki, A., Puré, E., Tsourkas, A. (2014). Nanoparticles functionalized with collagenase exhibit improved tumor accumulation in a murine xenograft model. *Particle & Particle Systems Characterization*, *31*(12), 1307–1312. http://doi.org/10.1530/ERC-14-0411.Persistent

Park, J. H., Saravanakumar, G., Kim, K., & Kwon, I. C. (2010). Targeted delivery of low molecular drugs using chitosan and its derivatives. *Advanced Drug Delivery Reviews*. http://doi.org/10.1016/j.addr.2009.10.003

Park, K., Kim, J. H., Nam, Y. S., Lee, S., Nam, H. Y., Kim, K., Park, J., Kim, I., Choi, K., Kim, S., Kwon, I. C. (2007). Effect of polymer molecular weight on the tumor targeting characteristics of self-assembled glycol chitosan nanoparticles. *Journal of Controlled Release*, *122*(3), 305–314. http://doi.org/10.1016/j.jconrel.2007.04.009

Patel Parul, K., Satwara Rohan, S., & Pandya, S. S. (2012). Bacteria aided biopolymers as carriers for colon specific drug delivery system: A review. *International Journal of PharmTech Research*, *4*(3), 1192–1214.

Pillai, G. (2014). Nanomedicines for Cancer Therapy : An Update of FDA Approved and Those under Various Stages of Development. *SOJ Pharm Pharm Sci*, *1*(2), 1–13. http://doi.org/10.15226/2374-6866/1/2/00109

Pujana, M. A., Pérez-Álvarez, L., Iturbe, L. C. C., & Katime, I. (2012). Water dispersible pH-responsive chitosan nanogels modified with biocompatible crosslinking-agents. *Polymer (United Kingdom)*, *53*(15), 3107–3116. http://doi.org/10.1016/j.polymer.2012.05.027

Qi, L., Xu, Z., & Chen, M. (2007). In vitro and in vivo suppression of hepatocellular carcinoma growth by chitosan nanoparticles. *European Journal of Cancer*, *43*(1), 184–193. http://doi.org/10.1016/j.ejca.2006.08.029

Raju, G. S. R., Benton, L., Pavitra, E., & Yu, J. S. (2015). Multifunctional Nanoparticles: Recent Progress in Cancer Therapeutics. *Chem. Commun.*, *51*(68), 13248–13259. http://doi.org/10.1039/C5CC04643B

Raval, M., Bande, D., Pillai, A. K., Blaszkowsky, L. S., Ganguli, S., Beg, M. S., & Kalva, S. P. (2014). Yttrium-90 radioembolization of hepatic metastases from colorectal cancer. *Frontiers in Oncology*, *4*(July), 120. http://doi.org/10.3389/fonc.2014.00120

Ravikumar, R., Peng, M. M., Abidov, A., Babu, C. M., Vinodh, R., Palanichamy, M., Choi, E, Y., Jang, H. (2016). Nanofibrous Polymers Blend of Fluorouracil loaded Chitosan- Hydroxy Ethyl Cellulose / Poly Vinyl Alcohol : Synthesis and Characterization, *8*(2), 295–306.

Rejman, J., Oberle, V., Zuhorn, I. S., & Hoekstra, D. (2004). Size-dependent internalization of particles via the pathways of clathrin- and caveolae-mediated endocytosis. *The Biochemical Journal*, *377*(Pt 1), 159–69. http://doi.org/10.1042/BJ20031253

Sanna, V., Pala, N., & Sechi, M. (2014). Targeted therapy using nanotechnology: Focus on cancer. *International Journal of Nanomedicine*, *9*(1), 467–483. http://doi.org/10.2147/IJN.S36654

Shang, L., Nienhaus, K., & Nienhaus, G. U. (2014). Engineered nanoparticles interacting with cells: size matters. *Journal of Nanobiotechnology*, *12*(1), 5. http://doi.org/10.1186/1477-3155-12-5

Sinha, R., Kim, G. J., Nie, S., & Shin, D. M. (2006). Nanotechnology in cancer therapeutics: bioconjugated nanoparticles for drug delivery. *Molecular Cancer Therapeutics*, *5*(8), 1909–1917. http://doi.org/10.1158/1535-7163.MCT-06-0141

Toden, S., Okugawa, Y., Jascur, T., Wodarz, D., Komarova, N. L., Buhrmann, C., Shakibaei, M., Boland, C. R., Goel, A. (2014). Curcumin mediates chemosensitization to 5-fluorouracil through miRNA-induced suppression of epithelialto-mesenchymal transition in chemoresistant colorectal cancer. *Carcinogenesis*, *36*(3), 355–367. http://doi.org/10.1093/carcin/bgv006

van Hazel, G. A., Heinemann, V., Sharma, N. K., Findlay, M. P. N., Ricke, J., Peeters, M., Perez, D.
Robinson, B. A., Strickland, A. H., Ferguson, T., Rodrigez, J., Kroning, H., Wolf, I., Ganju, V., Walpole, E., Boucher, E., Tichler, T., Shacham-Shmueli, E., Powell, A., Eliadis, P., Isaacs, R., Price, D., Moeslein, F., Taieb, J., Bower, G., Gebski, V., Van Buskirk, M., Cade, D. N., Thurston, K. Gibbs, P. (2016). SIRFLOX: Randomized Phase III Trial Comparing First-Line mFOLFOX6 (Plus or Minus Bevacizumab) Versus mFOLFOX6 (Plus or Minus Bevacizumab) Plus Selective Internal Radiation Therapy in Patients With Metastatic Colorectal Cancer. *Journal of Clinical Oncology*, *34*(15), 1–9. http://doi.org/10.1200/JCO.2015.66.1181

Veiseh, O., Sun, C., Fang, C., Bhattarai, N., Gunn, J., Du, K., Pullar, B., Lee, D., Ellenbogen, R. G. (2010). Specific targeting of brain tumors with an optical/MR imaging nanoprobe across the blood brain barrier, *69*(15), 6200–6207. http://doi.org/10.1158/0008-5472.CAN-09-1157.Specific

Venkatesan, P., Puvvada, N., Dash, R., Prashanth Kumar, B. N., Sarkar, D., Azab, B., Pathak, A., Kundu, S. C., Fisher, P. B., Mandal, M. (2011). The potential of celecoxib-loaded hydroxyapatite-chitosan nanocomposite for the treatment of colon cancer. *Biomaterials*, *32*(15), 3794–3806. http://doi.org/10.1016/j.biomaterials.2011.01.027

Ventola, C. L. (2012). The nanomedicine revolution: part 2: current and future clinical applications. *P & T : A Peer-Reviewed Journal for Formulary Management*, *37*(10), 582–91. Retrieved from http://www.pubmedcentral.nih.gov/articlerender.fcgi?artid=3474440&tool=pmcentrez&rendertype=abstract

Villegas, M. R., Baeza, A., & Vallet-Regí, M. (2015). Hybrid Collagenase Nanocapsules for Enhanced Nanocarrier Penetration in Tumoral Tissues. *ACS Applied Materials and Interfaces*, *7*(43), 24075–24081. http://doi.org/10.1021/acsami.5b07116

Weissig, V., Pettinger, T. K., & Murdock, N. (2014). Nanopharmaceuticals (part 1): products on the market. *International Journal of Nanomedicine*, *9*, 4357–4373. http://doi.org/10.2147/IJN.S46900

Xiong, W., Peng, L., Chen, H., & Qin, L. (2015). Surface modification of MPEG-b-PCL-based nanoparticles via oxidative self-polymerization of dopamine for malignant melanoma therapy. *International Journal of Nanomedicine*, *10*, 2985–2996. http://doi.org/10.2147/IJN.S79605

Xu, Q., Guo, L., Gu, X., Zhang, B., Hu, X., Zhang, J., Chen, J., Wang, Y., Chen, C ., Gao, B., Kuang, Y., Wang, S. (2012). Prevention of colorectal cancer liver metastasis by exploiting liver immunity via chitosan-TPP/nanoparticles formulated with IL-12. *Biomaterials*, *33*(15), 3909–3918. http://doi.org/10.1016/j.biomaterials.2012.02.014

Yang, S., Chen, J., & Shieh, M. (2008). Colorectal Cancer Cell Detection by Chitosan Nanoparticles Conjugated with Folic Acid 2-5 . Loading efficiency of indigo carmine in, *2*, 22–25.

Yang, S. J., Lin, F. H., Tsai, K. C., Wei, M. F., Tsai, H. M., Wong, J. M., & Shieh, M. J. (2010). Folic acid-conjugated chitosan nanoparticles enhanced protoporphyrin IX accumulation in colorectal cancer cells. *Bioconjugate Chemistry*, *21*(4), 679–689. http://doi.org/10.1021/bc9004798

Yang, S.-J., Shieh, M.-J., Lin, F.-H., Lou, P.-J., Peng, C.-L., Wei, M.-F., Yao, C-J., Lai, P-S., Young, T.-H. (2009). Colorectal cancer cell detection by 5-aminolaevulinic acid-loaded chitosan nanoparticles. *Cancer Letters*, *273*(2), 210–220. http://doi.org/10.1016/j.canlet.2008.08.014

Yoon, H. Y., Son, S., Lee, S. J., You, D. G., Yhee, J. Y., Park, J. H., Swierczewska, M., Lee, S., Kwon, I. C., Kim, S. H., Kim, K., Pomper, M. G. (2014). Glycol chitosan nanoparticles as specialized cancer therapeutic vehicles: sequential delivery of doxorubicin and Bcl-2 siRNA. *Scientific Reports*, *4*, 6878. http://doi.org/10.1038/srep06878

Zhu, X. L., Du, Y. Z., Yu, R. S., Liu, P., Shi, D., Chen, Y., Wang, Y., Huang, F. F. (2013). Galactosylated chitosan oligosaccharide nanoparticles for hepatocellular carcinoma cell-targeted delivery of adenosine triphosphate. *International Journal of Molecular Sciences*, *14*(8), 15755–15766. http://doi.org/10.3390/ijms140815755

Online sources

Bowel cancer statistics. Cancer research UK (2012). Accessed in 2016, available in http://www.cancerresearchuk.org/health-professional/bowel-cancer-statistics#heading-Zero

Colorectal Cancer. American Cancer Society (2016). Accessed in 2016, available in http://www.cancer.org/cancer/colonandrectumcancer/

8. APPENDIX

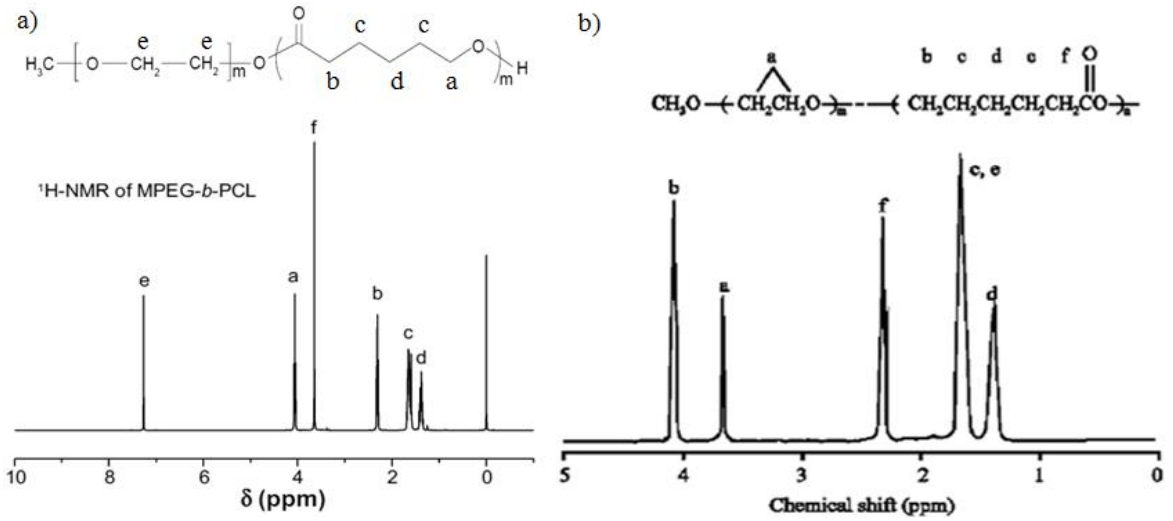

Figure 8.1 - ^{1}H-NMR spectrum obtained for mPEG-co-PCL and its corresponding chemical structure (represented by letters) by a) Xiong et al., 2015 and b) Baimark, 2009.

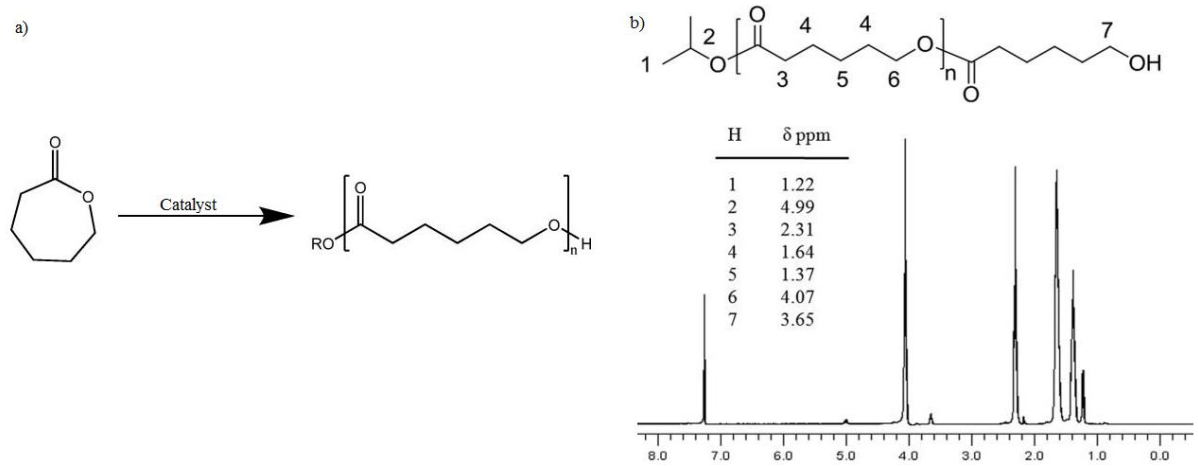

Figure 8.2 – a) Schematic representation of ε-caprolactone ring opening polymerization; b) NMR spectrum of poly(ε-caprolactone) and corresponding chemical groups. Adapted from Long et al., 2010.

'Wingardium leviosa'

Levita! Mais, sempre mais alto!

O mais longe que puderes…

*…**e mais além!***